学位論文

Development of an Optical Method to Control Temporal Patterns of a Protein Kinase Akt Activity Predictive with a Mathematical Model
（数理モデルを用いたタンパク質リン酸化酵素 Akt 活性の
時間パターン光操作法の開発）

平成２６年１２月　博士（理学）申請

東京大学大学院理学系研究科化学専攻

桂 嘉宏

Abstract

The dynamic spatiotemporal balance of various signaling pathways is crucial for living organisms. Of all the signaling pathways, Akt signaling pathway plays a key role in a variety of biological functions including glucose metabolism, cell differentiation, and protein synthesis. Abnormal patterns of Akt, such as hyper-activation and desensitization, cause numerous diseases including tumorigenesis and type II diabetes. In contrast to a switch-like response of a synaptic activity, Akt has a spatiotemporal gradient of its activity to generate its diverse functions. Therefore, the ability to control spatiotemporal Akt activity is crucial for elucidating the complicated physiological functions of Akt, yet no methods are currently available to allow such a flexible manipulation. (**Chapter 1**)

Herein, in the present thesis, I developed an optical system that has a potential to control spatiotemporal Akt activity. In the physiological condition, activation of Akt is triggered with its subcellular translocation from the cytosol to the plasma membrane in response to various extracellular stimulations. Based on the knowledge, I designed an optical system to manipulate Akt localization using a light-inducible protein interaction module of *Arabidopsis thaliana* photoreceptor Cryptochrome2 (CRY2) and its interacting partner protein CIB1. The Akt fused to a CRY2phr, which is a minimal light sensitive domain of CRY2 (CRY2-Akt), was reversibly activated by light illumination in the order of minutes within the physiological dynamic range and specifically regulated the downstream molecules and biological functions of gene expression and actin remodeling. (**Chapter 3**)

Furthermore, I generated a computational model to control the temporal patterns of CRY2-Akt activity in a precise quantitative manner. The constructed model and experimental results revealed that Akt is activated in a positive feedback loop mediated by phosphatidylinositide-3-kinase (PI3K) activation and actin reorganization. The constructed mathematical model correctly reproduced the CRY2-Akt response under genetic and

pharmacological perturbations, and allowed predictive control of the temporal CRY2-Akt activity. The optical module with computational modeling demonstrated a general framework for a predictive manipulation of optogenetic modules. Finally, as a demonstration of the developed method's utility, functional analysis of temporal patterns of Akt activity was conducted. (**Chapter 4**)

Materials and experimental details are described in **Chapter 2**. Final conclusion of this thesis is given in **Chapter 5**.

Chapter 1. General Introduction 1
1.1 Protein phosphorylation 2
1.2 Akt signaling pathway 4
1.3 Previous analytical methods of Akt biology 9
1.3.1 Methods to control Akt activity 9
1.3.2 Methods to visualize Akt activity 10
1.4 Optical methods to control biological functions 12
1.4.1 Photo-responsible tools 12
1.4.2 *Arabidopsis thaliana* photoreceptor Cryptochrome2 (CRY2) and CIB1 14
1.4.3 Quantitative manipulation of optical modules 16
1.5 Purpose of the present study 17
Chapter 2. Materials and Methods 18
2.1 Materials 19
2.2 Construction of plasmids for mammalian cell expression 19
2.3 Cell culture and retrovirus infection 19
2.4 Western blotting assay 20
2.5 Quantitative RT-PCR assay 20
2.6 Time-lapse imaging 23
2.7 PIP3 quantification by total internal reflection fluorescence microscopy (TIRFM) 24
2.8 Quantification of membrane ruffling and cell polarity 24
2.9 Computational modeling of CRY2-Akt activation 25
2.10 Statistical analysis 27
Chapter 3. Development of an Optical Method to Control Akt Activity 28
3.1 Development of an optical Akt module 29
3.2 Light-induced activation of CRY2-Akt 33
3.2.1 Specific and reversible activation of CRY2-Akt activity 33

3.2.2 Optimization of the intensity and duration of the light pulse 38
3.3 Optical control of biological functions of Akt 39
3.3.1 Optical control of FoxO functions 39
3.3.2 Optical control of actin remodeling 44
3.4 Discussion 46
3.5 Conclusion 48
Chapter 4. Predictive Control of Temporal Patterns of Akt Activity 49
4.1 General significance of the mathematical model construction 50
4.2 Mathematical modeling of temporal patterns of CRY2-Akt activity 51
4.2.1 Non-feedback model 51
4.2.2 Feedback model 55
4.3 Validation of the developed model and estimated parameters 58
4.3.1 Experimental confirmation of the feedback-mediated Akt activation 58
4.3.2 Qualitative validation of the developed model 64
4.3.3 Quantitative validation of the developed model 67
4.4 Functional analysis of the temporal patterns of Akt activity 69
4.5 Discussion 70
4.6 Conclusion 71
Chapter 5. General Conclusion 72
Acknowledgement 75
References 76

Chapter 1.
General Introduction

1.1 Protein phosphorylation

Protein phosphorylation, which is governed by a group of proteins called ‘protein kinase’, is one of the reversible post-translational protein modifications that contribute to control of various biological functions[1,2]. The phosphorylation induces conformational changes of phosphorylated substrate proteins and subsequent perturbation of downstream biological functions. Dephosphorylation is also controlled specifically by proteins called ‘protein phosphatase’, generating a reversibility of the phosphorylation events in living systems. In eukaryotic cells, only three amino acids, serine, threonine, and tyrosine that contain a nucleophilic hydroxyl group (-OH) at their side chains, are the phosphorylation targets in substrate proteins, but lipids, carbohydrates and nucleotides are also included in non-protein substrates. Interaction between the kinase and its substrate induces nucleophilic attack to the γ-phosphate group on adenosine triphosphate (ATP), resulting in transfer of the phosphate group to the substrates (**Fig. 1-1**). Each kinase or phosphatase has its own substrate specificity, but a redundancy of the relationship between enzyme and its substrate is a common mechanism in a physiological context, making it difficult to identify the specific functions of kinases and phosphatases[1]. In human genome, 518 kinases are encoded, constituting around 2.3% of all human genes[3,4]. Because of their diverse biological functions and connections to human diseases, the simple chemical reaction have gained intense interests of biological research.

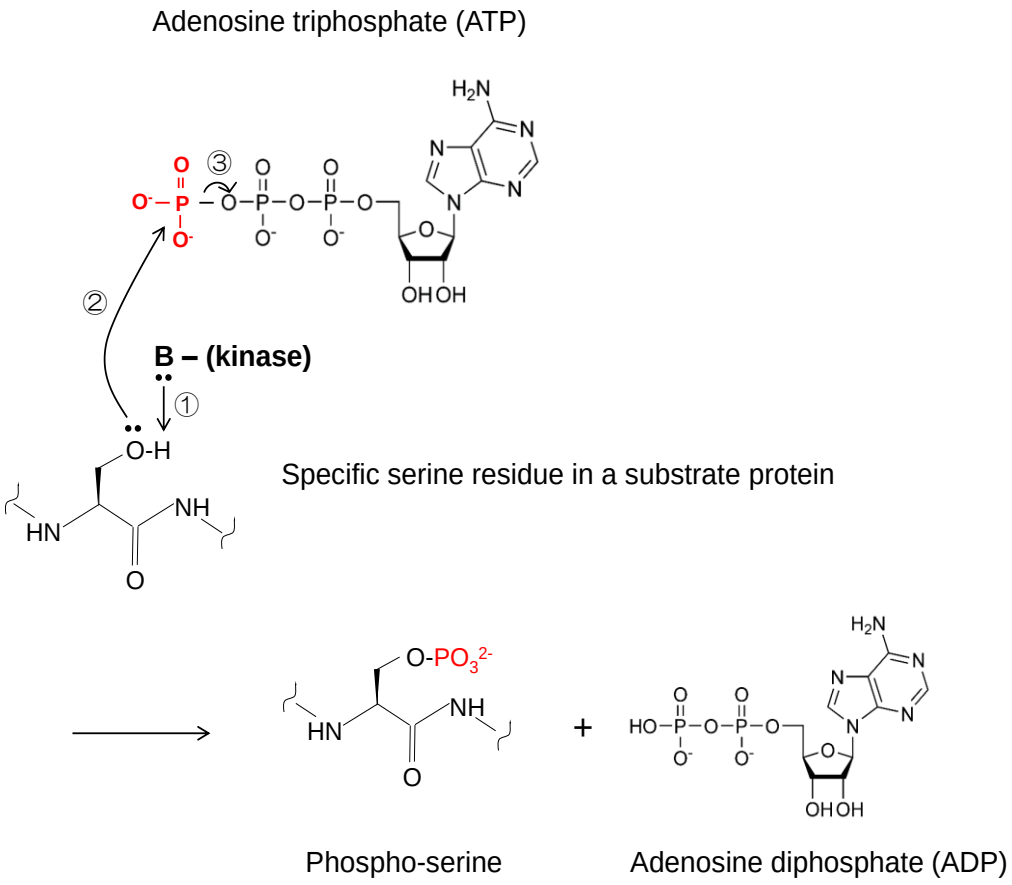

Figure 1-1. Mechanism of protein phosphorylation.
Kinase-catalyzed proton transfer from the (–OH) group on serine induces the nucleophilic attack of the γ-phosphate group on ATP, resulting in transfer of the phosphate group to serine to form phosphorylated serine (phospho-serine) and ADP. 'B' indicates the kinase-containing base that initiates proton transfer.

1.2 Akt signaling pathway

Akt also known as protein kinase B (PKB) is one of the serine/threonine kinases and is categorized as a member of AGC kinase family (i.e. protein kinases A, G, and C) that has a homologous catalytic kinase domain among them. Mammals have three structurally similar and approximately 80% sequence identical Akt isoforms, Akt1, Akt2, and Akt3. Those isoforms have different expression patterns in organs and tissues and have different substrate specificity with each other[5,6]. For example, in contrast to the relatively high expression of Akt3 only in neuronal cells, Akt1 and Akt2 are expressed in most of the cell types. Glucose metabolisms are mainly controlled by Akt2 isoform. However, the mechanisms that generate those differences among isoforms in spite of the similarity in catalytic domain are not fully understood. All isoforms are composed of two domains, pleckstrin homology (PH) domain and kinase domain[7] (**Fig. 1-2A**).

A conserved amino acid sequence of Akt phosphorylation was identified as R-X-R-X-X-S/T* by screening assays with a peptide library[8] and with mutations of a first-identified direct substrate protein of Akt, GSK-3[9], where R is arginine, S is serine, T is threonine, X is any amino acids, and * represents phosphorylation site. Based on such knowledge, previous studies have identified over 100 direct substrate proteins of Akt including FoxO, caspase-9, BAD, and eNOS[10]. Owing to their diverse biological functions, such as glucose metabolism, cell cycle, cell survival, angiogenesis, and cell differentiation, Akt is known as one of the most important central hub proteins in cellular signaling pathways (**Fig. 1-2B**). Furthermore, abnormal activity of Akt is implicated in the pathogenesis of a wide range of human diseases, such as type II diabetes, tumorigenesis, and neurodegenerative diseases[11]. Hence, the better understanding of Akt signaling is expected to provide a key to treat such human diseases.

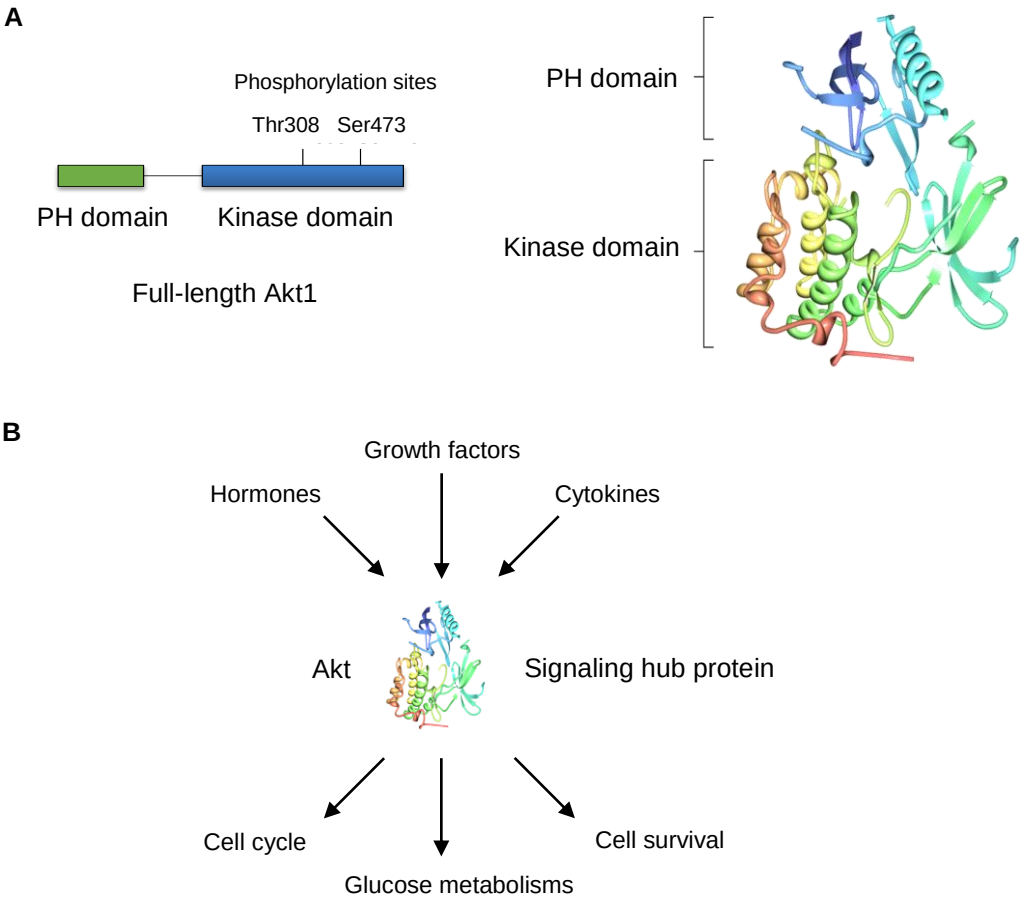

Figure 1-2. Protein structure and functions of Akt.
A. Primary and tertiary structure of Akt. Akt has two phosphorylation sites, Thr308 and Ser473 with numbering of Akt1 isoform. Akt2 is phosphorylated at Thr309 and Ser474 and Akt3 at Thr305 and Ser472. 3D structure of human Akt1 was resolved by X-ray cryptography[7]. PH domain: Pleckstrin Homology domain. Protein data bank (PDB) ID: 3O96. **B.** Kinase activity of Akt functions as a signaling hub by receiving various extracellular stimulations and transmitting the corresponding outputs to its substrate proteins.

The kinase activity of Akt is regulated through the phosphorylation at the kinase domain of Akt by upstream kinases, Thr308 by PDK1[12] and Ser473 by mammalian target of rapamycin complex 2 (mTORC2)[13] (amino acid numbering: Akt1 isoform) (**Fig. 1-3A**). Upon extracellular stimulations, such as growth factors, hormones, and cytokines, phosphatidylinositol 3-kinase (PI3K) is activated by a chain of biochemical reactions and produces a lipid molecule phosphatidylinositol 3,4,5-trisphosphate (PIP3) from phosphatidylinositol 4,5-bisphosphate (PIP2) (**Fig. 1-3B** and **Fig. 1-4**). By recognizing the cell membrane-bound PIP3 with its PH domain, Akt is translocated to the plasma membrane where it is activated by the upstream kinases. Translocation of the membrane-bound Akt to the cytosol is controlled through the hydrolysis of PIP3 by specific phosphatases, such as phosphatase and tensin homolog deleted from chromosome 10 (PTEN)[14]. Cytoplasmic Akt is inactivated (dephosphorylated) by specific phosphatases, Thr308 by protein phosphatase 2A (PP2A)[15] and Ser473 by PH domain and leucine rich repeat protein phosphatases (PHLPP)[16]. Three Akt isoforms have the same mechanism of activation and inactivation, yet the efficiency of cell membrane translocation was reported to differ depending on cell type[17], post-translational modifications[18], and genetic mutations[19].

The proper balance of phosphorylation and dephosphorylation is crucial and is often regulated in a spatiotemporal manner for generating appropriate biological outputs in response to extracellular inputs, which are also spatially and temporally controlled in living systems. Insulin, a secreted peptide hormone that controls glucose metabolism with activation of Akt, is known to have several distinct temporal secretion patterns from β-cells in pancreas[20,21]. By differently responding to the distinct temporal patterns of insulin secretion, Akt signaling is believed to maintain glucose metabolisms properly inside the living organisms[22,23]. Therefore, genetic mutations, which affect the phosphorylation balance of Akt signaling, are known as a prominent feature of insulin tolerance that causes type II diabetes[24]. Although the significance of such dynamic activity of insulin and Akt in living systems is implicated with an analysis of computational modeling, there is no direct experimental evidence to support the hypothesis,

because of the lack of methods to specifically reconstitute the physiological temporal patterns of Akt activity.

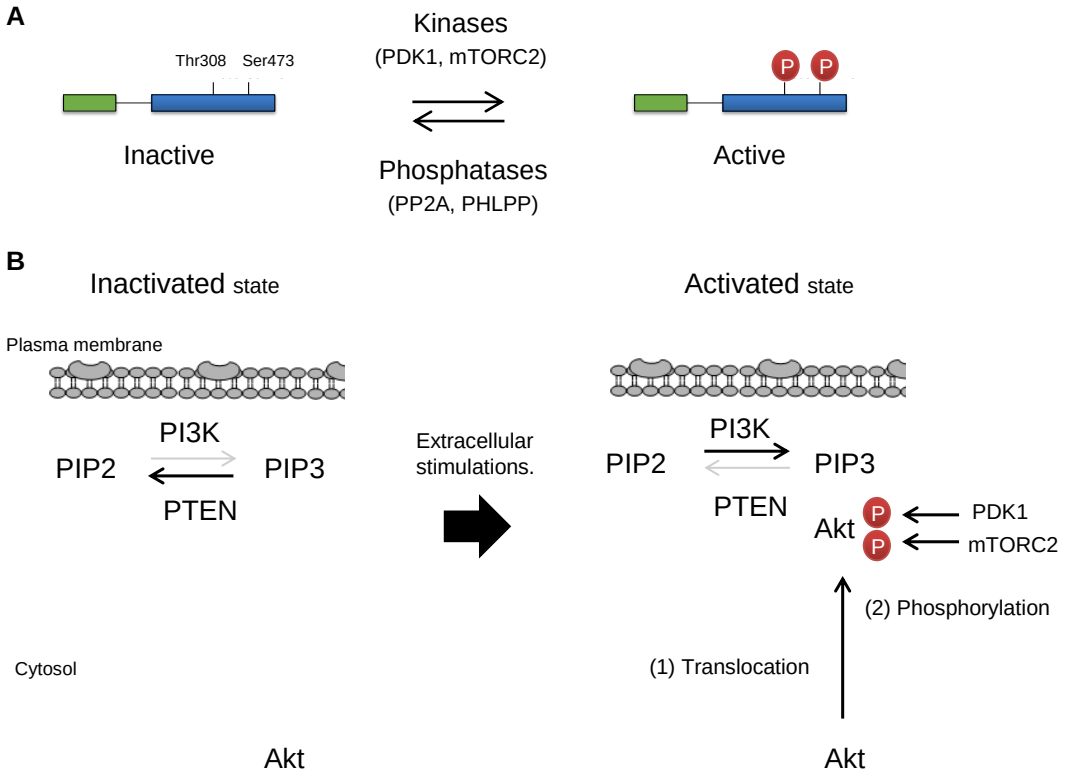

Figure 1-3. Mechanism of Akt activation.
A. The threonine and serine at the kinase domain are phosphorylated by kinases, PDK1 and mTORC2, and are dephosphorylated by phosphatases, PP2A and PHLPP, respectively. PH domain recognizes PIP3 which is synthesized by PI3K. 'P' indicates a phosphate group attached by kinases. **B.** Diagram of Akt activation. Activation of Akt is regulated by its membrane translocation and subsequent phosphorylation by its upstream kinases. Extracellular stimuli-induced PIP3 recruits Akt to the plasma membrane mediated by interaction between negative charge of PIP3 and positive charge of PH domain.

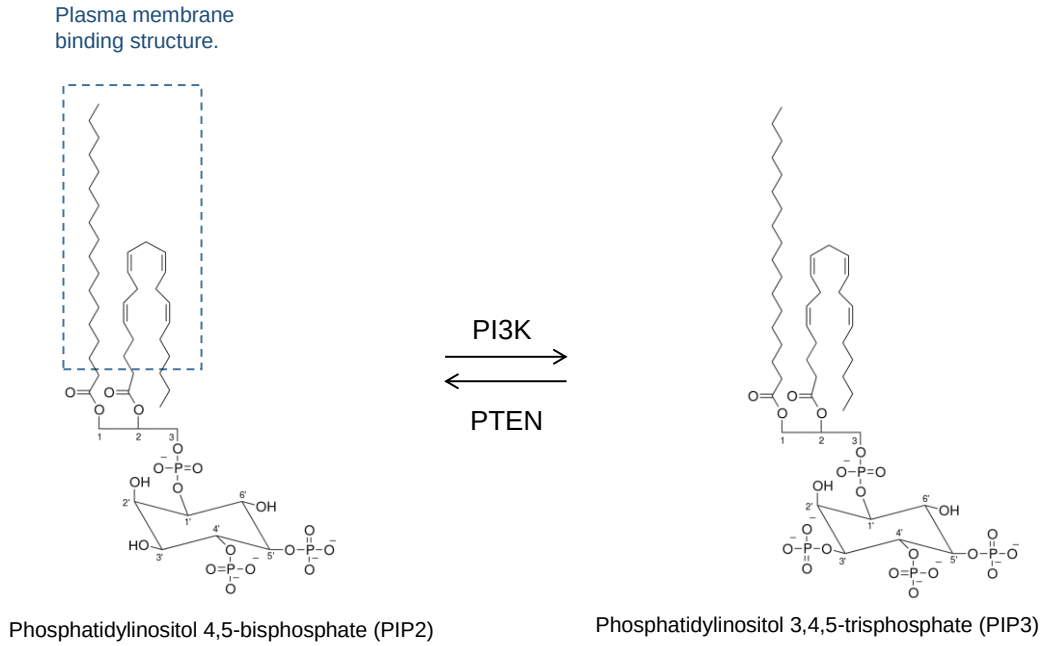

Figure 1-4. Mechanism of PIP2–PIP3 conversion.
PIP2 and PIP3 are composed of two domains, hydrophilic inositol ring locating in the cytosol and hydrophobic diacylglycerol embed in the cell membrane lipid bilayer. Upon extracellular stimulation such as growth factors, hormones, and cytokines, PI3K is activated, inducing the phosphorylation of PIP2 at the 3'-position of its inositol ring. Generated PIP3 recruits a set of PH domain-containing proteins including Akt. Conversion of PIP3 to PIP2 is controlled by PTEN phosphatase, which hydrolyzes the phosphate group at the 3'-position of its inositol ring.

1.3 Previous analytical methods of Akt biology

1.3.1 Methods to control Akt activity

Biological functions of Akt have been mainly investigated with genetic modifications and Akt-perturbing chemical compounds, both of which are classical and well-established methods. In genetic approaches, genetic modifications, such as gene-knockout or Akt mutant over-expression, are exploited to perturb Akt-regulated biological functions. Widely-used Akt mutants include a kinase-deficient Akt (Akt(K179M); a mutant containing lysine 179 substituted by methionine) that can't transfer phosphate group to substrate proteins[25], and a constitutively active Akt (Myr-Akt; a mutant attached with a cell membrane targeting signal sequence, Myr) that is persistently localized and active at the plasma membrane[26]. By comparing the phenotype of mutants with that of wild type of cells, tissues, or animals, specific functions of Akt activity have been explored. Similarly, in chemical compound-based approaches, reagents that have excitatory or inhibitory effects on Akt have been used to investigate the Akt-regulated functions. Because of the pharmaceutical needs, potent and specific Akt inhibitors have been extensively explored[27,28].

Although these methods are extremely effective in identifying the static function of Akt in population of cells, they are less effective to uncover the molecular dynamics of Akt activity in a single cell level because they have low spatiotemporal regularity. In order to investigate the functions of dynamic Akt activity, novel methods that have a potential to regulate spatiotemporal Akt activity in living subjects have been crucially necessitated.

1.3.2 Methods to visualize Akt activity

In contrast to the aforementioned classical approaches that enable to investigate Akt functions in population of cells, methods to visualize Akt activity in a single living cell have been developed to investigate dynamic activity of Akt with the advances of genetically-encoded light-emitting proteins, such as fluorescent proteins and luciferases[29–31]. The basis of these approaches is a conversion of the Akt-induced phosphorylation event into the change of biosensors' light emission property, such as the wavelength and the intensity of light. Biosensors based on a fluorescence resonance energy transfer (FRET) are a most common approach to detect phosphorylation in living subjects[32,33]. FRET biosensors are composed of four domains, a phosphorylation target mimetic sequence, its recognition motif in a phosphorylation-dependent manner, a donor fluorescent protein, and an acceptor fluorescent protein whose excitation spectrum overlap emission spectrum of the donor (**Fig. 1-5**). In the absence of Akt activity, excitation light of the donor fluorescent protein induces the fluorescence emission from the donor. On contrary, upon phosphorylation at the substrate mimetic sequence by Akt, the donor and the acceptor come close together within 10 nm, generating the FRET-induced fluorescence emission from the acceptor with the donor excitation. By using FRET biosensors, stimulus-induced dynamic activity of Akt was visualized in living cells and it was revealed that Akt activity is spatially and temporally controlled at subcellular compartments, such as Golgi apparatus, mitochondria, and nucleus[34–38]. Furthermore, visualization of Akt activity in living tumor-bearing mice was demonstrated with a genetically-encoded biosensor based on a luciferase technique[39].

These existing biosensors are crucially useful for observing the real-time dynamic activity of Akt and raises the next issue; what is the functional significance of such dynamic activity in living subjects. Because of the inability to artificially reconstitute such dynamic activity in living subjects, it is not fully understood how the observed spatiotemporal activity of Akt contributes to the whole biological systems.

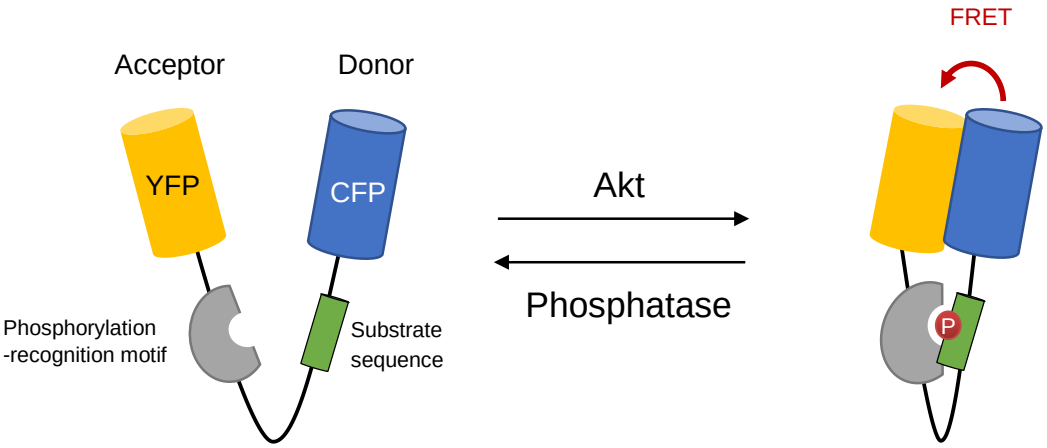

Figure 1-5. Visualization of spatiotemporal Akt dynamics using FRET biosensors.
FRET biosensors are composed of 4 domains, acceptor fluorescent protein, donor fluorescent protein, phosphorylation recognition motif, and substrate mimetic sequence. Typically, a cyan fluorescent protein(CYP) and a yellow fluorescent protein(YFP) are used for the donor and the acceptor, respectively. Upon phosphorylation at the substrate mimetic sequence by Akt, the phosphorylation recognition motif binds to the phosphorylated sequence, increasing the FRET efficiency between CYP and YFP.

1.4 Optical methods to control biological functions

1.4.1 Photo-responsible tools

Recently, a variety of photo-responsible tools has been applied to the functional analysis of biological events. Taking advantage of the ability to control the spatiotemporal patterns of light source, light-responsible tools opened a new avenue to perturb and analyze complicated biological systems with high spatiotemporal precision. These optical methods are categorized into two, chemical compound-based tools (called caged compounds) and genetically-encodable protein-based tools (called optogenetics).

Caged compounds are generally small organic molecules, whose bio-active structures are masked with a protecting group responsible to UV-light[40]. Upon UV-light absorption, these compounds release biomolecules, such as ATP[41], calcium ion[42], and mRNA[43], perturbing specific biological functions in a spatiotemporal manner. Of particular, caged-L-glutamate is one of the most successful examples of caged compounds in the studies of neuronal functions. It facilitated the functional analysis of the relationship between the activity in a specific spatial region in neuron and its function. Caged compounds provide a sophisticated approach to investigate the functions of specific biomolecules with high spatiotemporal resolution, yet the technique has several limitations, such as the irreversibility of photoreaction, the toxicity of UV-light, and the toxicity of byproducts derived from caging group. Additionally, in some cases, cell membrane disruption is required to load caged compounds into living subjects.

Optogenetics is an emerging technique in the field of biotechnology. It is based on light-sensitive proteins, most of which are originated from plants. By genetically modifying photo-receptors themselves or fusing protein of interest with them, optical manipulation of diverse biological events, such as ion flux in neurons[44,45], protein–protein interaction[46,47], protein clustering[48–50], gene expression[46,51], and cell motility[52,53] were demonstrated. In contrast to the aforementioned caged compounds, the photo-reaction is triggered by visible light in most

optogenetic tools instead of the relatively cytotoxic UV-light. In addition, the genetically-encodable feature of the optogenetic modules enables them to be easily expressed inside living cells and animals by conventional gene transfer techniques or genome editing techniques. Channelrhodopsin[54,55], Cryptochrome2 (CRY2)[46], and Phytochrome[56,57] are one of the most widely used photo-receptors, which have different photo-response properties with each other such as absorption spectrum, photo-cycle kinetics, and the ability to interact with other proteins in a light-dependent manner.

1.4.2 *Arabidopsis thaliana* photoreceptor Cryptochrome2 (CRY2) and CIB1

Cryptochromes are photolyase-like proteins that regulate photomorphogenic development in plants and circadian clock both in plants and mammals. Instead of the light absorption property of plant cryptochromes, mammalian cryptochromes evolutionally lost their photo-sensitivity. An application of the plant *Arabidopsis thaliana* Cryptochrome2 (CRY2) to the optogenetics in mammalian cells was first described in 2012, in which authors demonstrated optical manipulation of gene expression based on a light-induced dimerization between CRY2 and its interacting partner protein, CIB1[46]. The dimerization occurs within 1 s upon light illumination at a wavelength of 400–500 nm. The complex dissociates within 5–10 min in a dark condition, enabling a reversible control of biological events. The optogenetic system does not require addition of an exogenous cofactor, because of the existence of chromophore, flavin adenine dinucleotide (FAD), in mammalian cells. Light absorption results in electron transfer to oxidized FAD, which induces the conformational change of the Cryptochromes (**Fig. 1-6, A and B**). Although the photo-cycle of the chromophore was partially revealed with *in vitro* spectroscopic studies[58,59], the mechanism of light-triggered electron transfer is controversial. Also, the mechanisms of conformational change of the photoreceptor are largely unknown.

The CRY2–CIB1 module has enabled the optical control of several fundamental biological processes such as phosphoinositide metabolism[60,61], endogenous transcription and epigenetic states[62], organelle transport[63], and the activity of extracellular signal-regulated kinase (ERK)[64], demonstrating the broad applicability of the methodology to the manipulation of living systems.

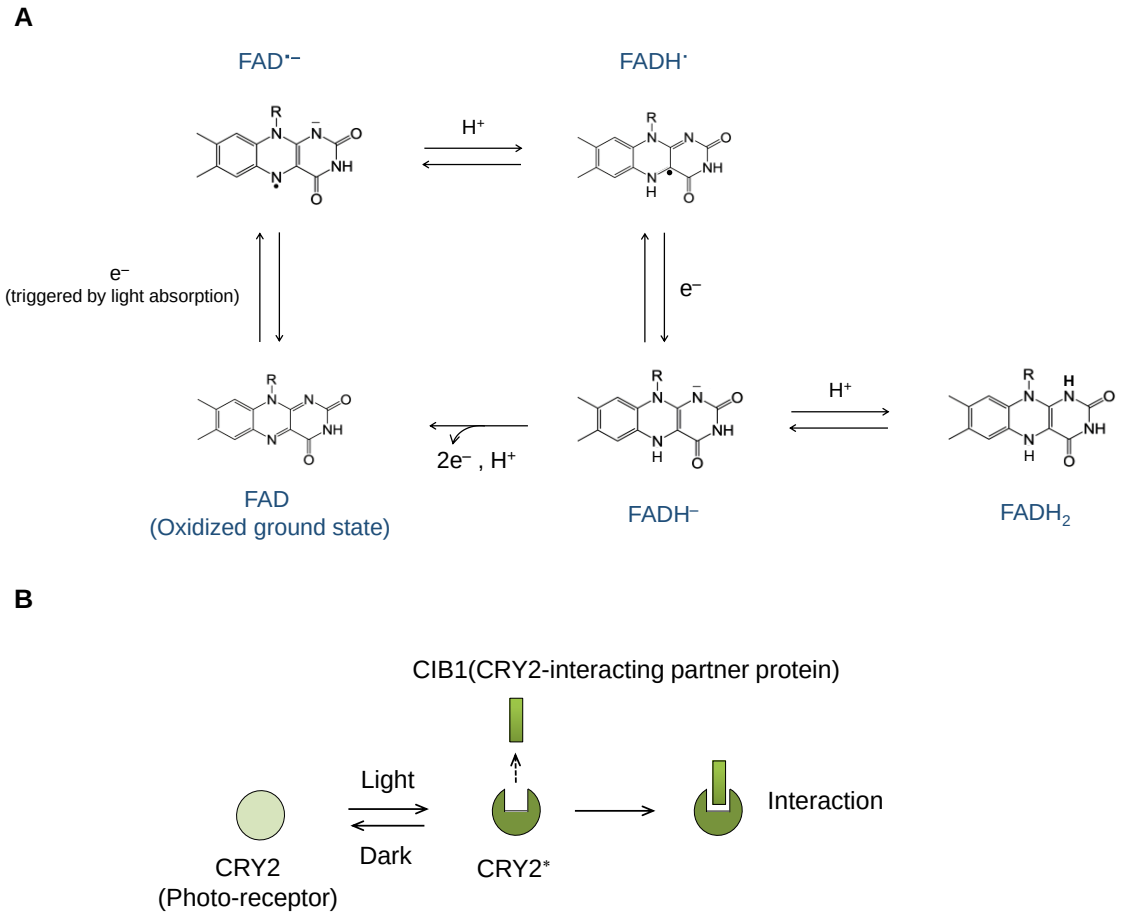

Figure 1-6. A photoreceptor protein, Cryptochrome2 (CRY2) and its chromophore, FAD. **A.** Photo-cycle of CRY2 chromophore, flavin adenine dinucleotide (FAD). In live cells, FAD is maintained in the oxidized form by dissolved oxygen. The ground state FAD is cable of absorbing light effectively. Light illumination triggers electron transfer to FAD. Reduced FAD triggers conformational change of the photo-receptor. The diagram was modified based on the figure 1(a) in the paper, Liu, H., Liu, B., Zhao, C., Pepper, M. & Lin, C. "The action mechanisms of plant cryptochromes.", *Trends Plant Sci*. 16, 684–91 (2011). **B.** Light-induced interaction between photo-receptor CRY2 and its-interaction partner protein CIB1. Absorption of light ranging from 400–500 nm induces conformational change of CRY2, resulting in the interaction with CIB1.

1.4.3 Quantitative manipulation of optical modules

Increasing demonstrations of optogenetic approaches highlight that the genetically-encoded light-responsible tools are a promising technique to apply precise biological inputs to living subjects. However, at present, a lack of general framework to *quantitatively* manipulate optical tools prevents its broad applicability. It is totally unclear how the light should be illuminated to achieve the desired activity of optogenetic tools. Rounds of optimization of light illumination protocol are required in each of the optogenetic application. One method to address this issue is the use of an on-line feedback system, in which optogenetic output is adjusted in real time with fluorescence monitoring[65,66]. However, this method lacks generality owing to the limitation of selecting florescent dyes and proteins, because optogenetic systems preclude the use of fluorophores with absorption spectra that overlap the spectra of the optogenetic modules. In addition, the strategy is not applicable to the optical manipulation faster than several minutes, because of the delay time required for analyzing obtained images and searching optimized parameters of light input. Those difficulties in the existing strategy limit its general applicability to broad optical tools and necessitates an alternative approach to manipulate optical tools quantitatively.

1.5 Purpose of the present study

Akt is one of the most important signaling hub proteins, whose dynamic activity has been investigated with methods such as biochemical assays and genetically-encoded fluorescent reporters. Although the dynamic activity of Akt is suggested to be crucial to determine cellular outcome, it is currently unclear how and to what extent the Akt activity dynamics contribute to the functions of whole living systems. The ability to control Akt activity using light is expected to facilitate the elucidation of the complicated physiological functions of Akt in living subjects. Considering such a huge need, I aimed to develop an optical method to regulate Akt activity using a photo-receptor that forms a dimer upon light absorption. By using the designed optical system, optical control of Akt activity and Akt-regulated biological functions were demonstrated.

Furthermore, in combination with a mathematical model that describes the dynamics of optical module, I aimed to establish a general framework to manipulate optical tools in a precise predictive manner. Although optogenetic manipulations provide a huge potential to investigate fundamental biological processes in detail, the inability to control optogenetic output in a precise quantitative manner limits the anticipated potential at the present stage.

Chapter 2.
Materials and Methods

2.1 Materials

Specific antibodies for pAkt(Thr308)(#2965), pAkt(Ser473)(#4051), Akt(#4691), pGSK3α/β(S21/9)(#9331), GSK3(#5676), p-ERK1/2(T202/Y204)(#4370), ERK1/2(#4695), and PTEN(#9559) were obtained from Cell Signaling Technology. VO-OHpic and Wortmannin were obtained from Sigma Aldrich. Insulin, LatrunculinB, and LY294002 were obtained from Wako Pure Chemical Industries.

2.2 Construction of plasmids for mammalian cell expression

The cDNAs encoding human Akt1/PKBα (Original ORF clone: ORK02215; Kazusa), human PTEN (Original ORF clone: FXC09870; Kazusa), CRY2 and CIB1 (Addgene) used for the plasmid construction were amplified by a standard PCR with gene specific primers. The membrane-targeting myristoylation and palmitoylation signal sequence (MGCVQCKDKEATKLTE) originated from the sequence of Fyn. The respective efficiencies of membrane translocation were almost equal for full-length CRY2 and CRY2PHR (amino acids 1–498), as described previously[46]. Point mutations were introduced by mutagenic complement oligo single-stranded DNA pairs. These constructs were inserted into pcDNA vectors (Invitrogen) for transient expression in mammalian cells or the pMX vector for retrovirus infection.

2.3 Cell culture and retrovirus infection

C2C12, HEK293, and PlatE cells were maintained in DMEM supplemented with 10% FBS, 100 units/ml penicillin, and 100 μg/ml streptomycin at 37 °C in 5% CO2. For retrovirus infection to C2C12 cells, plasmid DNA was transfected with TransIT-LT1 reagent (Takara) into packaging cells (PlatE cells). After 2 days of culture, high-titer retroviruses were collected and

used to infect C2C12 cells. To achieve high expression level of the optical modules, multiple rounds of infection were conducted in 6-h intervals. Cells were seeded onto 35-mm dishes for Western blotting assays and onto 24-well plates for quantitative RT-PCR assays.

2.4 Western blotting assay

Prior to the assays, the culture medium of C2C12 cells in 35-mm dish was replaced with phenol red-free DMEM supplemented with 0.1%FBS and carefully maintained in the dark overnight at 37 °C in 5% CO2. The serum-starved cells were stimulated with light pulses using a blue-LED transilluminator (470 nm, LEDB-SBOXH; Optocode) and then lysed with 200 μL of sampling buffer (5% SDS, 10% glycerol, 10% 2-mercaptoethanol, 125 mM Tris-HCl, pH 6.8) and gently sonicated for 3–5 min. Insoluble debris was removed by centrifugation at 15,000 × g at 4 °C for 15 min. The sample was boiled at 95 °C for 5 min and separated on SDS-polyacrylamide gels. The electrophoreticall separated proteins were transferred onto PVDF membranes (GE Healthcare) and blocked with 1% skimmed-milk in Tris-buffered saline containing Tween-20 (TBS-T: 150 mM NaCl, 0.05% Tween-20, 50 mM Tris-HCl, pH 8.0) for at least 1 h and subsequently immunoblotted with specific antibodies. The immunoblotted bands were detected using ECL detection reagents with an image analyzer (LAS-1000; Fuji Film or LAS-4000; GE Healthcare). The intensity of immunoblotted bands was measured using the ImageJ software. It was possible to activate the present system with sustained light illumination. However, a pulse light illumination protocol was adopted in this study to rapidly activate CRY2-Akt with the minimal effects due to chromophore bleaching and photo-toxicity.

2.5 Quantitative RT-PCR assay

For RT-PCR, cells in each well of 24-well plates were stimulated using a custom LED

array controlled by a microcontroller (Arduino UNO). LEDs (470 nm, 60° illumination, OptoSupply) were placed underneath wells of a 24-well plate to stimulate the cells in each well with an independent illumination protocol at an intensity of 1 mW/cm^2 (**Fig. 2-1**). Although 4 mW/cm^2 intensity of light achieved fastest activation of CRY2-Akt, the condition yielded a large variable in the expression level of an internal control gene cyclophilin A (particularly at the time point of 270 min), probably because of the cytotoxicity of light illumination. Therefore, in the quantitative RT-PCR assays, which required longer duration of light illumination, I adopted 1 mW/cm^2 intensity, at which expression level of the internal control gene was relatively stable. The cells were fixed with 300 μL of RNA later (Qiagen) and total RNA was isolated using the Agencourt RNAdvance Tissue kit (Beckman Coulter). The isolated RNAs were reverse transcribed to cDNAs by the PrimeScript RT reagent Kit (Takara), and measured by the real-time quantitative RT-PCR with gene-specific primers (*Atrogin-1*: forward [5'-CAGCTTCGTGAGCGACCTC-3'] and reverse [5'-GGCAGTCGAGAAGTCCAGTC-3'], *cyclophilin A*: forward [5'- GAGCTGTTTGCAGACAAAGTTC-3'] and reverse [5'-CCCTGGCACATGAATCCTGG-3']). I calculated the relative abundance of *Atrogin-1* mRNA using *cyclophilin A* mRNA as an internal control. PCR reactions were performed using SYBR Premix Ex TaqII (Takara) in a Thermal Cycler Dice Real-time system TP-800 (Takara).

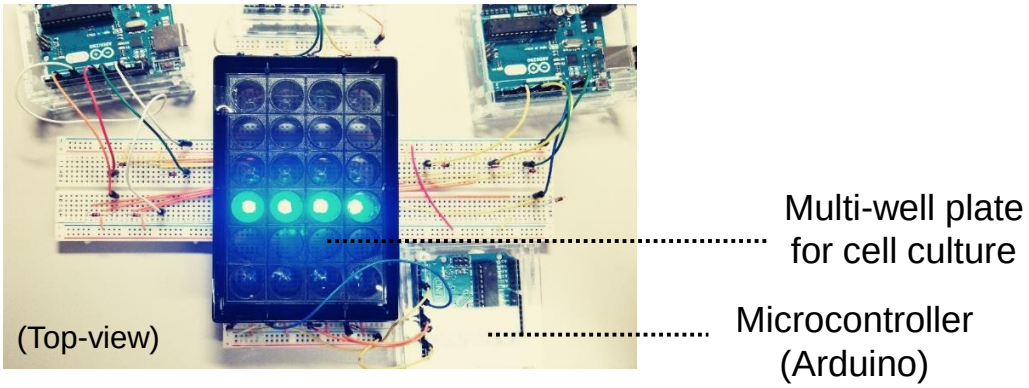

Figure 2-1. Custom-built LED array system for flexible temporal light illumination.
Cells in each well of 24-well plates were stimulated using a custom LED array controlled by a microcontroller, Arduino UNO. LEDs (470 nm, 60° illumination, OptoSupply) were placed underneath wells of a 24-well plate to stimulate cells in each well with an independent illumination protocol. The cells were subjected to quantitative RT-PCR assays.

2.6 Time-lapse imaging

In the assays to evaluate the light-dependent translocation of CRY2-Akt, HEK293 cells or C2C12 cells were seeded onto a 35-mm glass-bottom dish in phenol red-free DMEM supplemented with 10% FBS, 100 unit/mL penicillin and 100 μg/mL streptomycin. Twenty-four hours after incubation at 37 °C in 5% CO_2, the cells were transfected with plasmid DNAs. Two days after transfection, the cells were observed using a confocal fluorescence microscope (FV1000-D; Olympus) with a PlanApo 60×oil immersion objective (N.A.: 1.35), 515-nm laser for Venus excitation, and 559-nm laser for mCherry excitation. The illumination power for photo-activation of CRY2-Akt was 0.5–3.0%, with a 20 mW 440-nm laser light at a speed of 2.0 μs/pixel. For FoxO1-mCherry translocation assays, C2C12 cells expressing Myr-CIBN and CRY2-Akt were seeded onto a 35-mm glass-bottom dish. Then, the cells were transfected with a plasmid encoding FoxO1-mCherry after 24 h of incubation. After an additional 24 h of incubation, the cells were starved with phenol red-free DMEM supplemented with 0.1% FBS and carefully maintained in the dark overnight at 37 °C in 5% CO_2. Activation of CRY2-Akt was conducted with 1-min intervals of 440-nm laser light 6–12 times in the middle of each experiment. The expression of Myr-CIBN and CRY2-Akt was confirmed at the end of the assays, because exposure of the excitation light for fluorescent proteins perturbs CRY2-Akt activity. The fluorescence intensity at cytosol and nucleus was quantified using the ImageJ software. The N/C ratio change was calculated by dividing an average N/C ratio after light stimulation by the ratio prior to light stimulation. The 440-nm wavelength of laser light for the photo-activation in the time-lapse imaging assays was different from the 470-nm wavelength of LED light used for the western blotting assays and quantitative RT-PCR assays because of the limitation of the microscopic setup. Because absorption spectrum of the photoreceptor CRY2 was broad, (ranging from 400–500 nm), both wavelengths of light were functional in activating the optogenetic system. In the present stage, it was not problematic to activate the system with two different light sources that had

different activation efficiencies, because I did not directly compare the data from single cells to that from cell populations.

2.7 PIP3 quantification by total internal reflection fluorescence microscopy (TIRFM)

Cells expressing Akt-SNAPf were treated with 10 nM tetramethylrhodamine (TMR)-conjugated SNAPf ligands for 20 min and washed three times with PBS. The cells were serum-starved overnight in HBSS containing 0.1% FBS and subjected to the PIP3 quantification assay. Single molecule imaging of Akt-SNAPf(TMR) was performed using an inverted microscope (IX-81; Olympus), equipped with a home-build TIRF apparatus, a 561 nm laser and a PlanApo 100×oil immersion objective (N.A.: 1.45). Fluorescence signals from TMR were detected with a cooled EM-CCD camera (ImagEM; Hamamatsu photonics). Aquacosmos and HC-Image softwares (Hamamatsu photonics) were used to control the microscope system and to capture the fluorescence images, respectively. The Images were taken at a speed of 30 frame per second and a total of 100 frame images were analyzed. Light illumination was conducted using Blue-LED apparatus that generated a 2 mW/cm^2 intensity of 470 nm light at the sample point. The obtained images were analyzed with the ImageJ plugin Particle Tracker. Number of detected molecules was normalized to the images prior to stimulations.

2.8 Quantification of membrane ruffling and cell polarity

Membrane ruffling was quantified as previously described[67]. In short, the extent of ruffling of each cell was scored using a scale of 1–3, where 1 denotes that no ruffle was observed, 2 denotes that ruffling formation was confined to isolated regions covering ≤25% of the peripheral area, and 3 denotes that extensive ruffles were observed, covering >25% of the peripheral area. Cells with a score of 3 before light stimulation were excluded from analysis. The ratio of the

ruffling index (before light /after light) was calculated for >25 cells. Cells were stimulated with 440-nm laser 12 times at 1-min intervals under a microscope. For quantification of cell polarity, C2C12 cells expressing the optogenetic module and Lifeact-RFP were stimulated with single 440-nm laser pulse under a confocal microscope. To calculate the polarity index ($\cos\theta$) of the migrating C2C12 cells, the x and y coordinates were obtained for the centroid before movement, the centroid after movement, and for the center of the irradiation spot by analyzing the Lifeact-RFP image using the ImageJ software.

2.9 Computational modeling of CRY2-Akt activation

I developed a light-dependent Akt activation model based on the law of mass action and performed simulation and parameter estimations using Matlab (R2012b) and the Systems Biology Toolbox 2 (SBTOOLBOX2) for MATLAB (**Fig. 2-2**). The parameters in the model were estimated using experimental data from **Fig.4-2** according to two methods in series: First, a meta-evolutionary programming method was used to approach the neighborhood of the local minimum. Second, the Nelder–Mead method was used to reach the local minimum[68]. After 200 independent estimations for the model, I selected the model that had the minimum value for the objective function, which was defined as the sum of the squared residuals between the experimentally obtained results and the simulations (**Fig. 2-3**).

$$\text{Objective Function Value} = \sum_{i} (Sim._i - Exp._i)^{1/2}$$

Note that the pathways and molecules in the model do not directly correspond to the real biochemical pathway because of the abstract model. I estimated the model parameters from experimentally obtained results of Thr308 of CRY2-Akt because the time course of Ser473 was nearly the same as that of Thr308. A model comparison was conducted using the Akaike Information Criterion (AIC) value[69] from each model. The AIC value was defined as follows.

$$\mathrm{AIC} = \ln\left(\frac{\mathrm{RSS}}{N}\right) + \frac{2m}{N}$$

Therein, N denotes the number of data points, m denotes the number of estimating parameters, and RSS denotes the residual sum of squares.

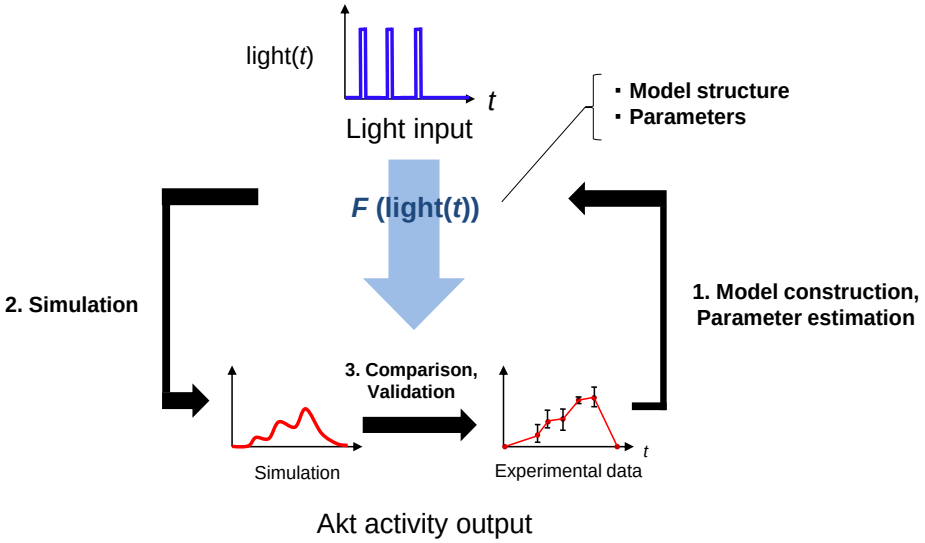

Figure 2-2. Schematic of the procedure of mathematical model construction.

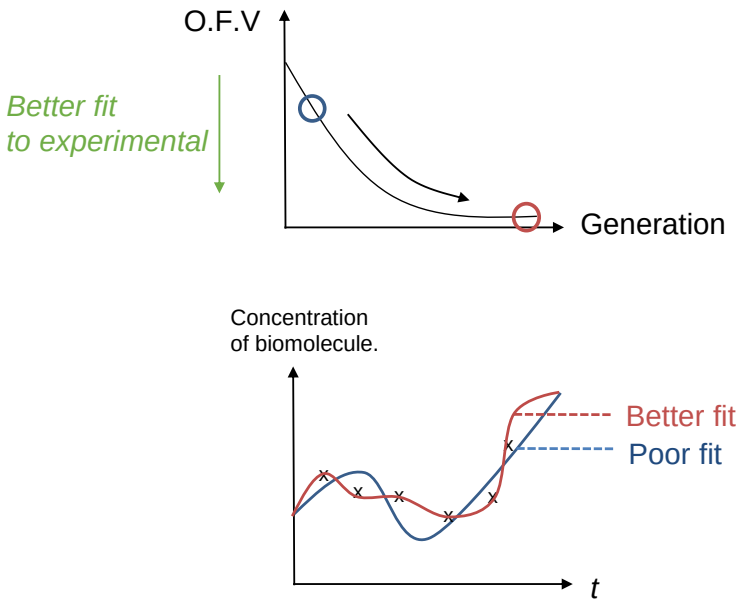

Figure 2-3. Schematic of the parameter estimations based on the evolutionally programming. (Upper) Decreasing O.F.V. as generation goes on. In evolutionally programming, a set of parameters are randomly mutated and the better set of parameters, which has lower O.F.V. survives in each generation.

2.10 Statistical analysis

Data are presented as the mean ± standard error of the mean (S.E.M.). Statistical significance was determined using unpaired or paired student's *t*-tests (two-tailed). *P* values <0.05 were considered as statistically significant.

Chapter 3.
Development of an Optical Method to Control Akt Activity

3.1 Development of an optical Akt module

To generate a photo-activatable Akt (PA-Akt), I tested three light-inducible systems using a CRY2–CIB1 dimerization system[46] (**Fig. 3-1A** and **Fig. 3-3, A and B**). It is previously reported that CRY2 transiently interacts with CRY2-interacting partner protein, CIB1 in a light dependent manner. Based on the criterion that the system must enable control of the Akt localization reversibly with minimal domains, I chose a system in which the kinase domain of Akt was fused with CRY2phr, a minimal light-sensitive domain of CRY2 (named CRY2-Akt), and the N-terminal portion of CIB1 (CIBN) was fused with a membrane targeting myristoylation sequence (named Myr-CIBN) (**Fig. 3-1, A and B**). The N-terminal glycine residue in the sequence is attached with a lipid myristate by an intracellular protein, *N*-myristoyltransferase to be localized at the cell membrane. To minimize the activation of the optogenetic module without light, only the kinase domain of Akt was fused with CRY2phr, because full-length of Akt contains PH domain responsible for PIP3 binding.

Myr-CIBN and CRY2-Akt were labeled with the yellow fluorescent protein Venus and the red fluorescent protein mCherry, respectively. Those fusion constructs were expressed in HEK293 cells by transfection and their localizations were examined with a confocal fluorescent microscope. In a dark condition, the Myr-CIBN was located at the plasma membrane of HEK293 cells; in contrast CRY2-Akt was localized in the cytosol. The CRY2-Akt was translocated to the plasma membrane upon stimulation of 440-nm light pulse without external cofactor addition (**Fig. 3-2A**). The kinetics were similar to those previously reported for CRY2–CIB systems[46] (**Fig. 3-2B**). In addition, the localization was regulated with subcellular resolution (**Fig. 3-2C**).

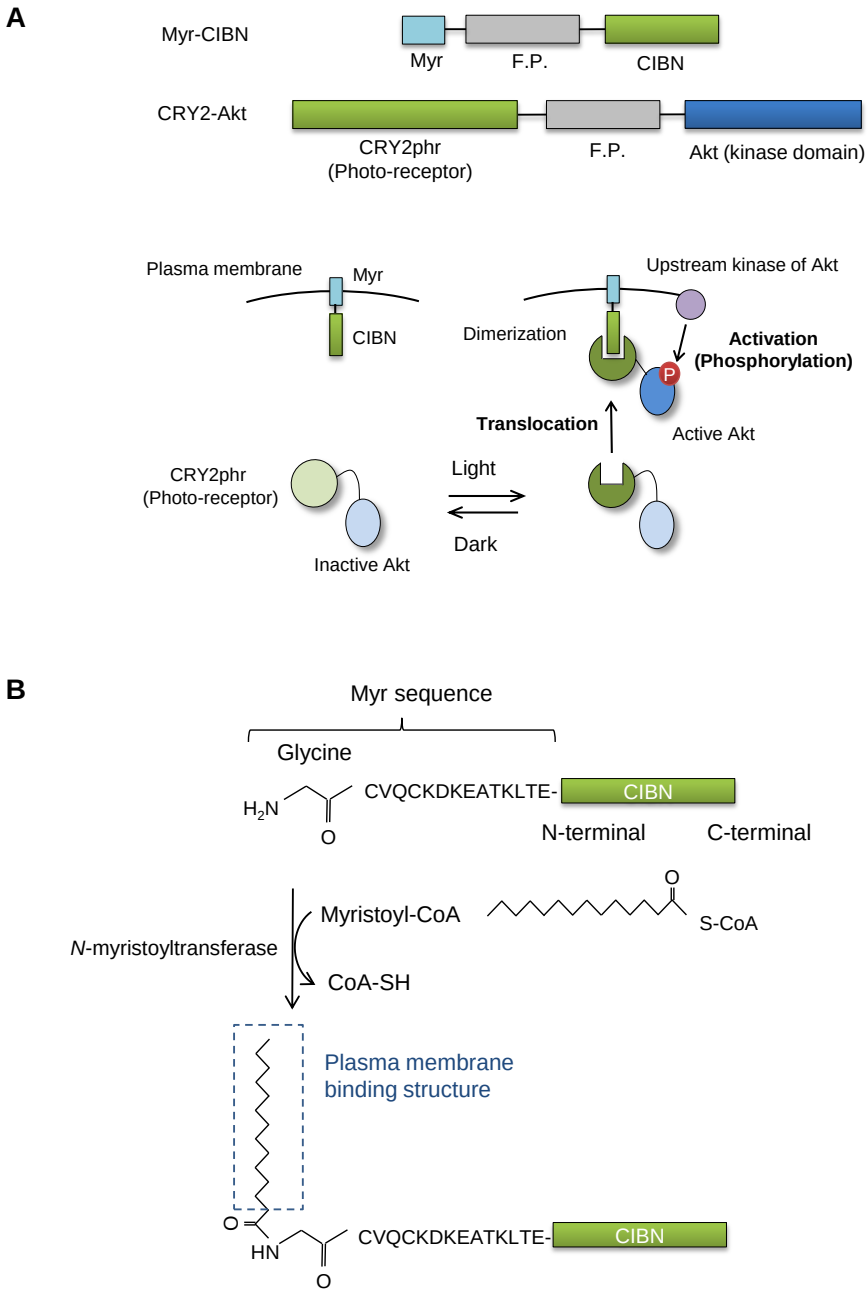

Figure 3-1. Principle of an optimized PA-Akt system.
A. Schematic of the optimized optical Akt module. CIBN is constitutively localized at the plasma membrane by fusing a membrane-targeting myristoylation signal sequence, Myr. Photo-receptor CRY2 is fused with a kinase domain of Akt. Light illumination results in the reversible interaction between CRY2 and CIBN, localizing Akt in the plasma membrane. F.P.: Fluorescent protein. **B.** Principle of cell membrane binding CIBN. Myr signal sequence is composed of 13 amino acids, whose first Glycine is posttranslationally modified by intracellular enzyme, *N*-myristoyltransferase, generating the motif of plasma membrane binding.

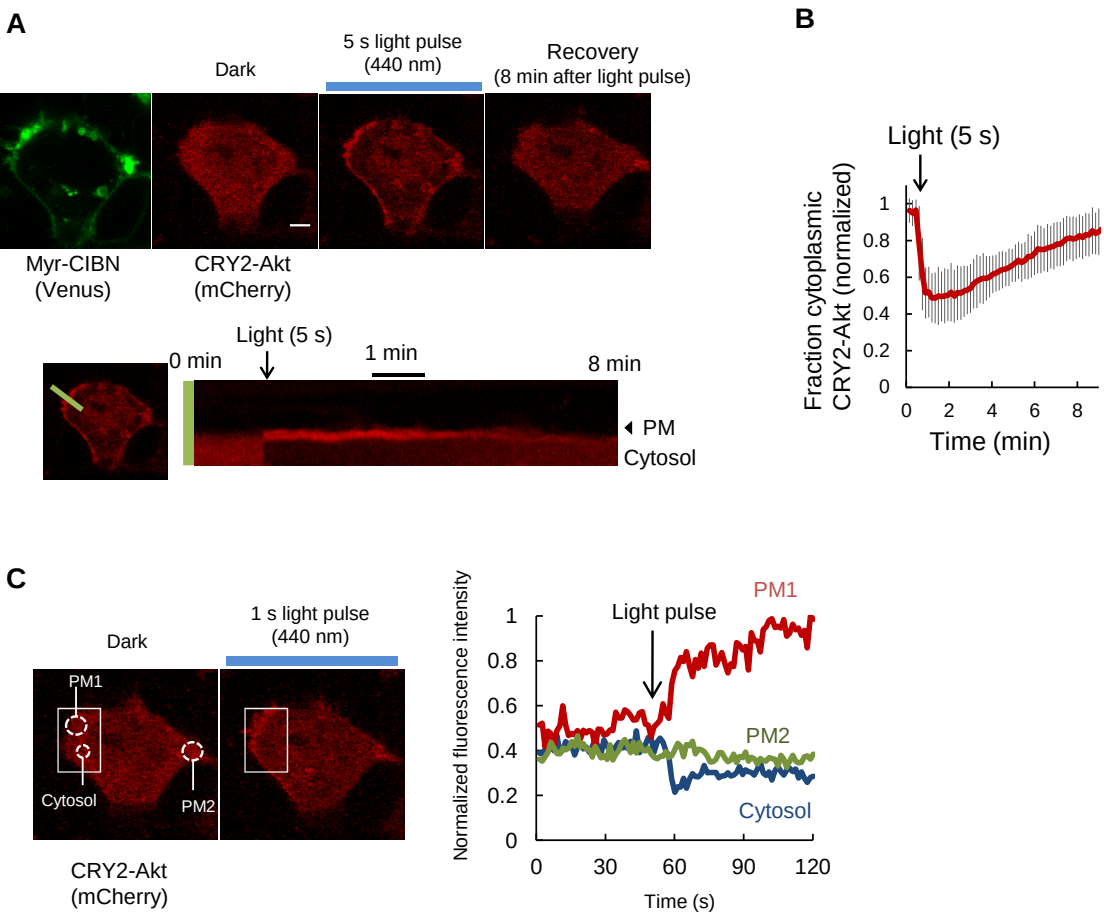

Figure 3-2. Light-induced membrane localization of CRY2-Akt in the optimized system. **A.** Light-induced membrane localization of CRY2-Akt in HEK293 cells. The cell expressing CRY2-Akt and Myr-CIBN was stimulated with 440-nm laser light for 5 s. A kymograph shows the change of fluorescence intensity of CRY2-Akt over 8 min along the green line in the left image: green, Myr-CIBN; red, CRY2-Akt; scale bar, 5 μm. **B.** A graph shows the time course of normalized fluorescence intensity of CRY2-Akt at cytoplasm. Bars: Mean ± S.D. (*N*=19). **C.** Subcellular control of CRY2-Akt localization in the same cell as shown in A. Square region was stimulated with 440-nm laser light for 1 s. Graph shows the time courses of normalized fluorescence intensity per pixel at three different regions in the cell. PM1: Plasma membrane at light-stimulated region. PM2: Plasma membrane at non-stimulated region. Cytosol: cytosol

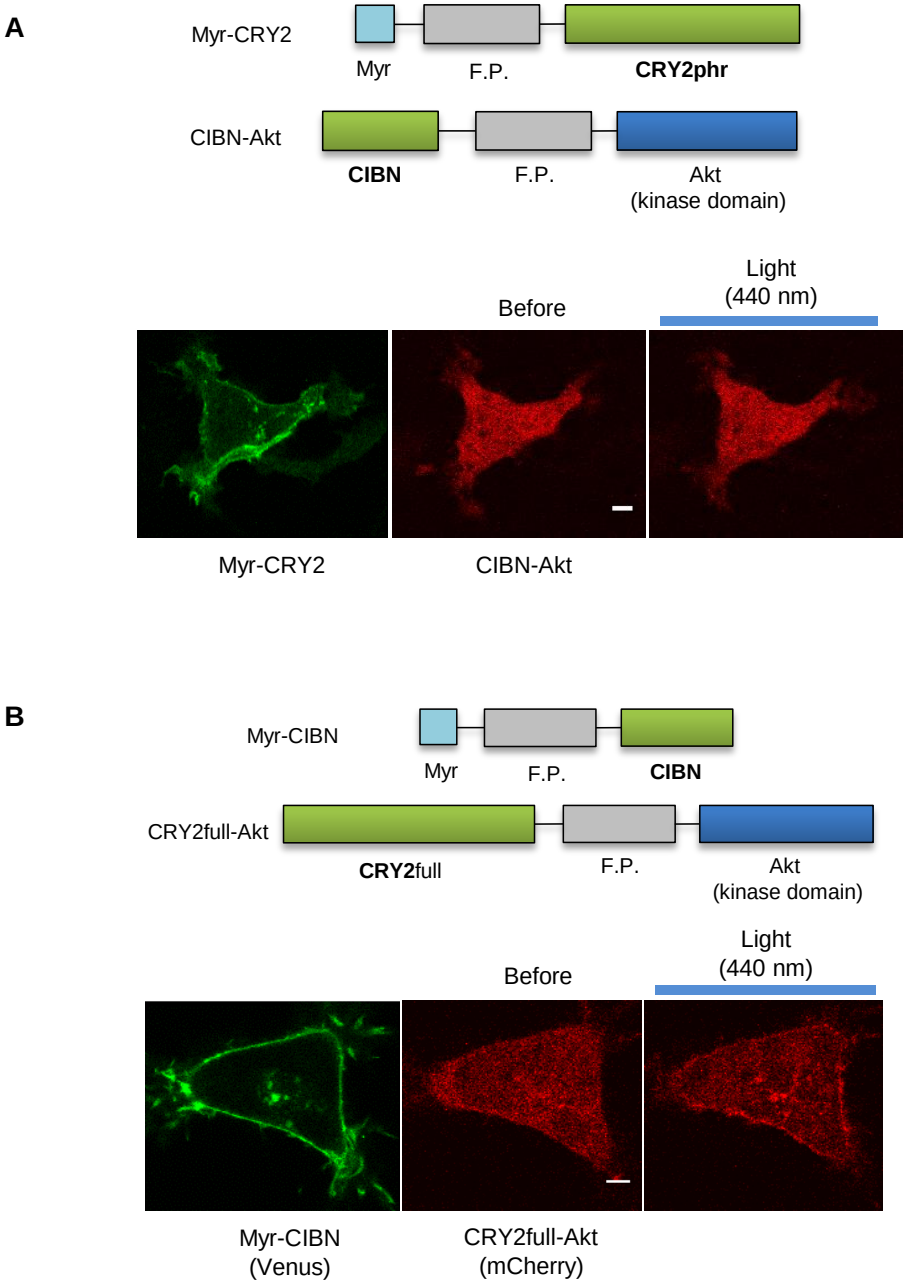

Figure 3-3. Optical systems tested through the optimization of PA-Akt system.
A. CIBN-Akt was not recruited to the cell membrane upon light in the cells expressing Myr-CRY2 and CIBN-Akt. CRY2 was localized at the plasma membrane by fusing the membrane targeting myristoylation sequence. Green: Myr-CRY2, Red: CIBN-Akt. Scale bar: 10 μm. **B.** Full-length CRY2 (CRY2full) was used as a dimerization domain with CIBN. The photoreaction kinetics is approximately the same as a CRY2phr. Green: Myr-CIBN, Red: CRY2full-Akt. Scale bar: 10 μm.

3.2 Light-induced activation of CRY2-Akt

3.2.1 Specific and reversible activation of CRY2-Akt activity

To evaluate activation of the membrane-localized CRY2-Akt, its phosphorylation at Thr308 and Ser473 was investigated in C2C12 cells expressing Myr-CIBN and CRY2-Akt by a biochemical assay, western blotting. The phosphorylation level increased directly with repeated pulses of 470-nm light and reached a plateau following more than 12 pulses (**Fig. 3-4, A and B**). The optogenetic constructs were introduced by retrovirus infection to decrease the variability of expression level of the constructs among the cells. The increased phosphorylation was also detected in the system containing the full-length of Akt (**Fig. 3-5**). The dynamic range of the phosphorylation was set to the comparable level to those of endogenous Akt and constitutively membrane-localized Akt (Myr-Akt) (**Fig. 3-6**). Termination of the light stimulation caused CRY2-Akt inactivation within tens of minutes and further light stimulation caused repeated activation (**Fig. 3-7**). Kinase activity of the phosphorylated CRY2-Akt was confirmed by the phosphorylation of the direct Akt substrate, Glycogen synthase kinase 3 (GSK3). Importantly, unlike insulin stimulation, which simultaneously activates several pathways including Akt and ERK, light stimulation achieved specific activation of Akt signaling (see the p-ERK1/2 column in **Fig. 3-4B**). Interestingly, specific Akt activation resulted in the reduced phosphorylation of ERK, which is consistent with a previous report[70].

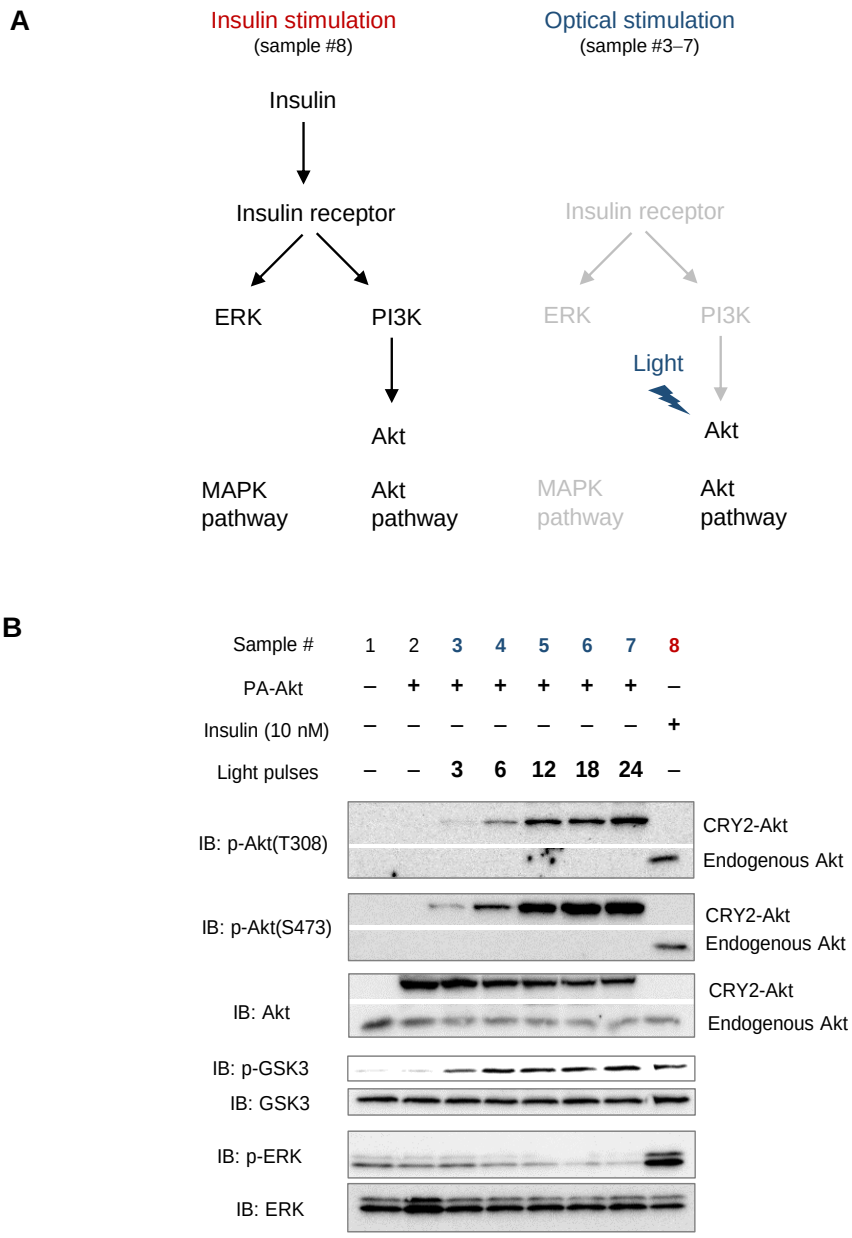

Figure 3-4. Specific activation of Akt signaling with light stimulation.
A. Comparison of chemical stimulation and optogenetic simulation. In chemical stimulation such as insulin, several pathways are simultaneously activated, making it difficult to reveal specific functions of Akt signaling. In contrast, optogenetic approach enables to specifically activate the Akt signaling. **B.** The experimental result of western blotting assay of light-illuminated cells expressing CRY2-Akt and Myr-CIBN. Cells were illuminated with different times of light pulses at 1 min interval. One-minute post final light illumination, the cells were collected and subjected to western blotting assay. Insulin was added for 10 min at a concentration of 10 nM. Glycogen synthase kinase 3 (GSK3) is a direct substrate of Akt. IB: Immunoblotting.

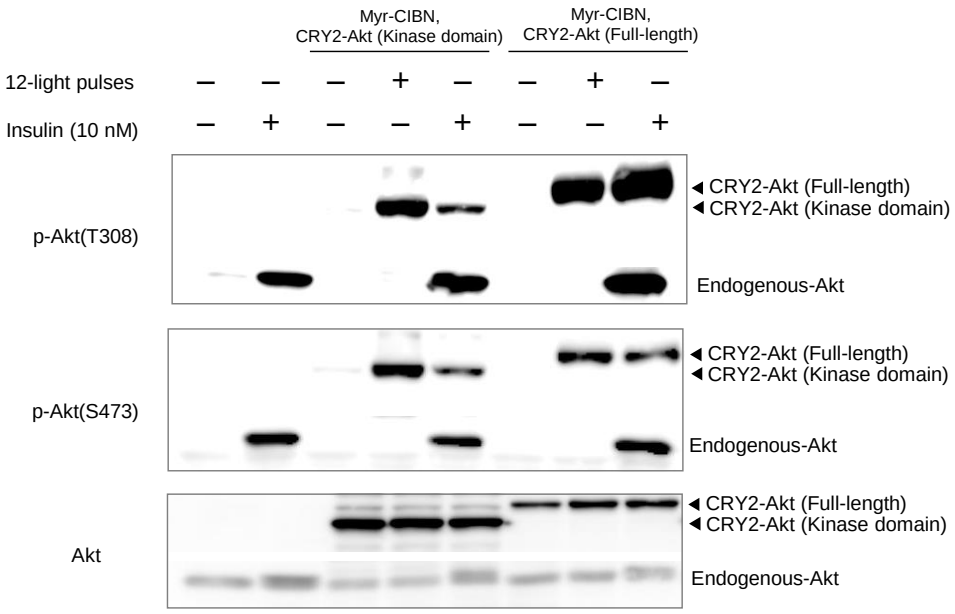

Figure 3-5. Comparison of the CRY2-Akt(Kinase domain) and the CRY2-Akt(Full-length). Activation of CRY2-Akt with light or insulin. Cells were treated with 12-light pulses at 1-min interval or with 10 nM insulin for 10 min. The degree of T308 phosphorylation with insulin was weaker in CRY2-Akt(Kinase domain) than in CRY2-Akt(Full-length), enabling specific activation with light illumination.

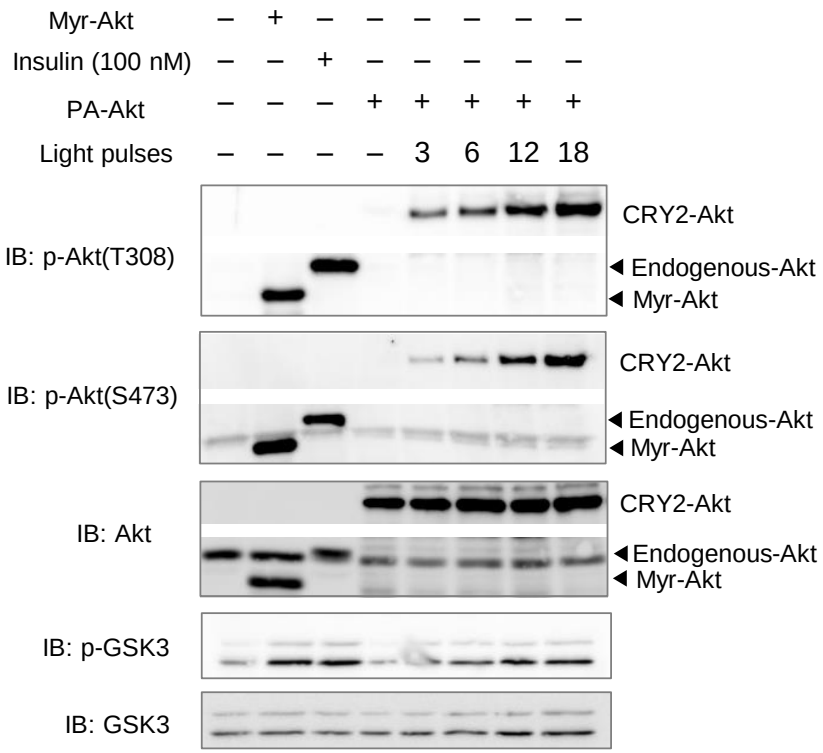

Figure 3-6. The dynamic range of CRY2-Akt activity.
CRY2-Akt was activated in a comparable level to a constitutively membrane-localized Akt (Myr-Akt) and endogenous Akt. Endogenous Akt was maximally activated with 100 nM insulin for 10 min.

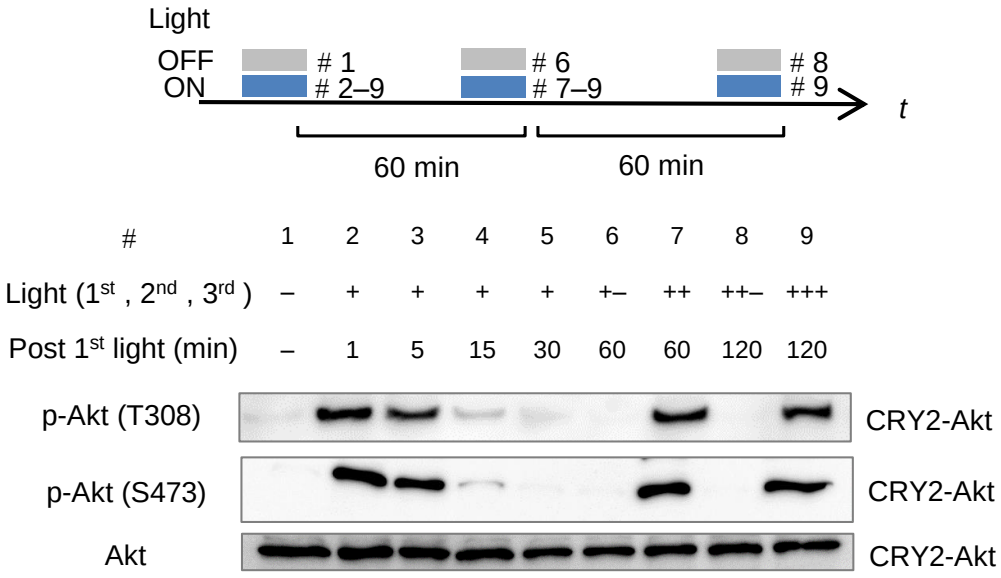

Figure 3-7. Reversibility of CRY2-Akt activation.
CRY2-Akt was activated three times each at an interval of 60 min. In each activation, cells were stimulated 12 times with light pulses at 1 min interval.

3.2.2 Optimization of the intensity and duration of the light pulse

To activate CRY2-Akt rapidly, the light intensity and duration were optimized. Cells expressing CRY2-Akt and Myr-CIBN were illuminated with light at an intensity of 1 mW/cm^2, 4 mW/cm^2, or 8 mW/cm^2 for 1-s or 5-s duration per minute and subjected to western blotting assays (**Fig. 3-8**). In each fixed condition of light intensity and duration, CRY2-Akt was phosphorylated in proportion to the number of light pulses. Rapid activation of CRY2-Akt was achieved in the illumination protocol of 4 mW/cm^2 intensity for 5-s duration. The illumination protocol was adopted in the following western blotting assays.

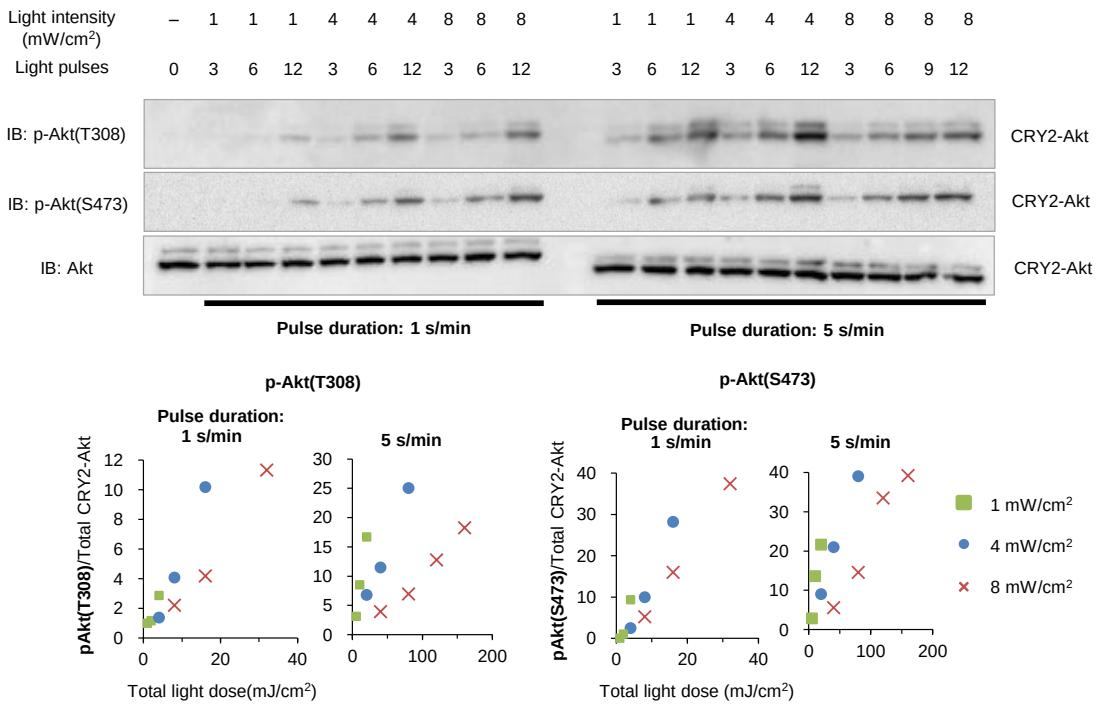

Figure 3-8. Optimization of the intensity and duration of the light pulse.
Light-induced phosphorylation of CRY2-Akt was evaluated in different light intensity, duration, and the times of pulses. Serum-starved C2C12 cells expressing Myr-CIBN and CRY2-Akt were stimulated with light pulses. The cells were collected 1 min after final light pulse and subjected to western blotting analysis. Activation intensity was approximately proportional to the times of light pulses in all light conditions. The maximum activation was achieved in the cells stimulated with 4 mW/cm^2 intensity for 5 s duration per minute. Graphs show the relative CRY2-Akt activity calculated from the immunoblotting band intensity. The total light dose was defined as a multiplicative result of intensity, duration, and times of light pulses.

3.3 Optical control of biological functions of Akt

3.3.1 Optical control of FoxO functions

To further characterize the present system, the perturbation of downstream biological processes of Akt was examined. The transcriptional factor FoxO1 is a key regulator of cell metabolism and its subcellular localization is controlled by Akt-mediated phosphorylation[71,72] **(Fig. 3-9)**. FoxO1 (labeled with mCherry) was co-expressed with Myr-CIBN (labeled with the enhanced cyan fluorescent protein ECFP) and CRY2-Akt (labeled with Venus) in C2C12 cells. Nuclear-localized FoxO1-mCherry was translocated to the cytosol upon light illumination (**Fig. 3-10, A and B**). Interestingly, Akt activation caused oscillations in nuclear abundance of FoxO1-mCherry in 5 of the 32 analyzed cells (**Fig. 3-11**), as observed in another transcriptional factor, NF-κB[73,74]. In addition, the expression level of FoxO1-regulated gene, muscle-specific ubiquitin ligase *Atrogin-1*[75–77], decreased 90 min after the onset of light illumination, but the amplitude of the decrease at the later time points was smaller in light-stimulated cells than in cells stimulated with insulin (**Fig. 3-12**). These results underscore the central role of Akt in regulating FoxO1 activity compared with other factors, such as FoxO1 acetylation, ubiquitination, and phosphorylation by other kinases[78], which would be necessary for a full decrease in *Atrogin-1* expression. In addition, I confirmed that the expression of Myr-CIBN and CRY2-Akt itself did not significantly alter the basal level of *Atrogin-1* expression, whereas the basal localization of FoxO1-mCherry was slightly affected by the expression of those constructs (**Fig. 3-13**). The results indicate that the over-expressed CRY2-Akt with Myr-CIBN might have a quite weak activity, causing nuclear export of the FoxO1-mCherry to a small extent.

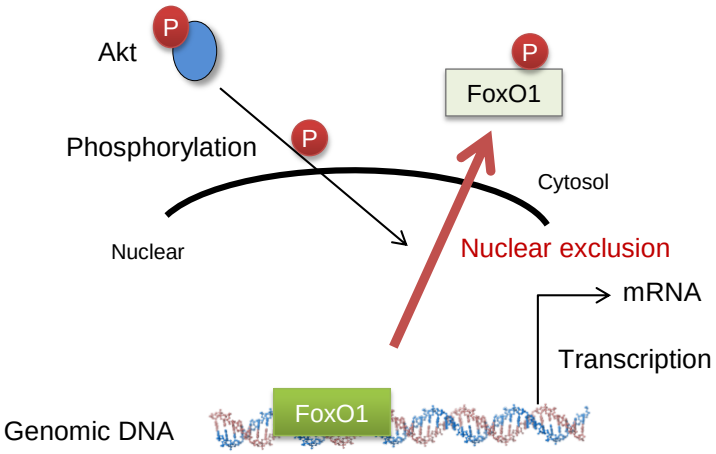

Figure 3-9. Nuclear exclusion of FoxO mediated by Akt-induced phosphorylation.
FoxO is a transcriptional factor that regulates expression of genes responsible for versatile cellular events including metabolism, differentiation, and survival. Akt excludes FoxO1 from nucleus by phosphorylating FoxO1 at Thr24, Ser256, and Ser319.

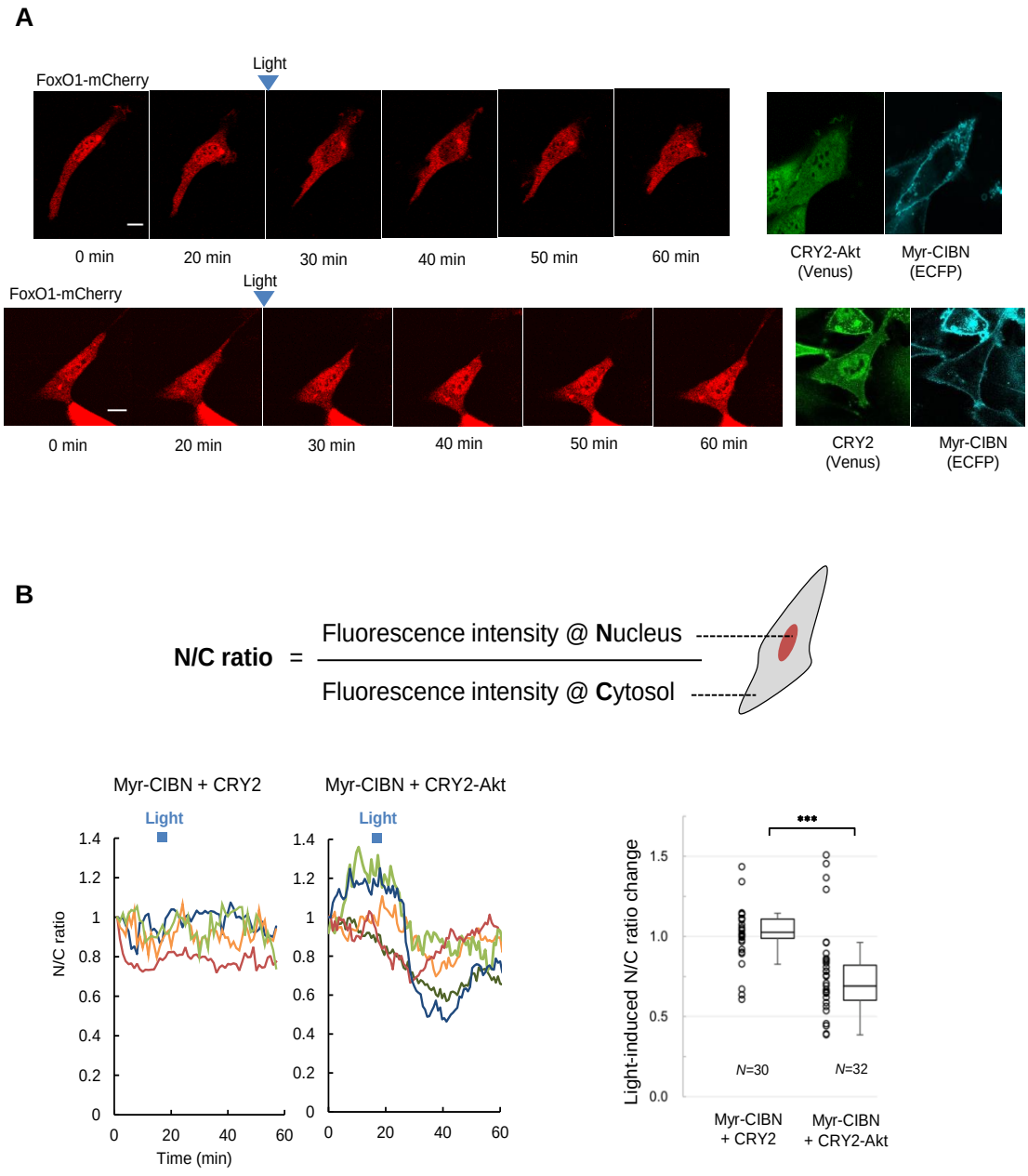

Figure 3-10. Optical control of FoxO1 nuclear exclusion.

A. Time-lapse images of FoxO1 upon CRY2-Akt activation in C2C12 cells. Myr-CIBN was labeled with ECFP, and CRY2-Akt with Venus. Scale bars: 10 μm. **B.** (Left) Representative time-course of Nuclear/Cytoplasm (N/C) fluorescence ratio of FoxO1-mCherry. (Right) Box and whisker plot of the N/C ratio change upon light illumination with outliers. (*N*=30 for control cells expressing Myr-CIBN and CRY2, *N*=32 for cells expressing Myr-CIBN and CRY2-Akt, *** p<0.001 by a two-tailed student's *t*-test).

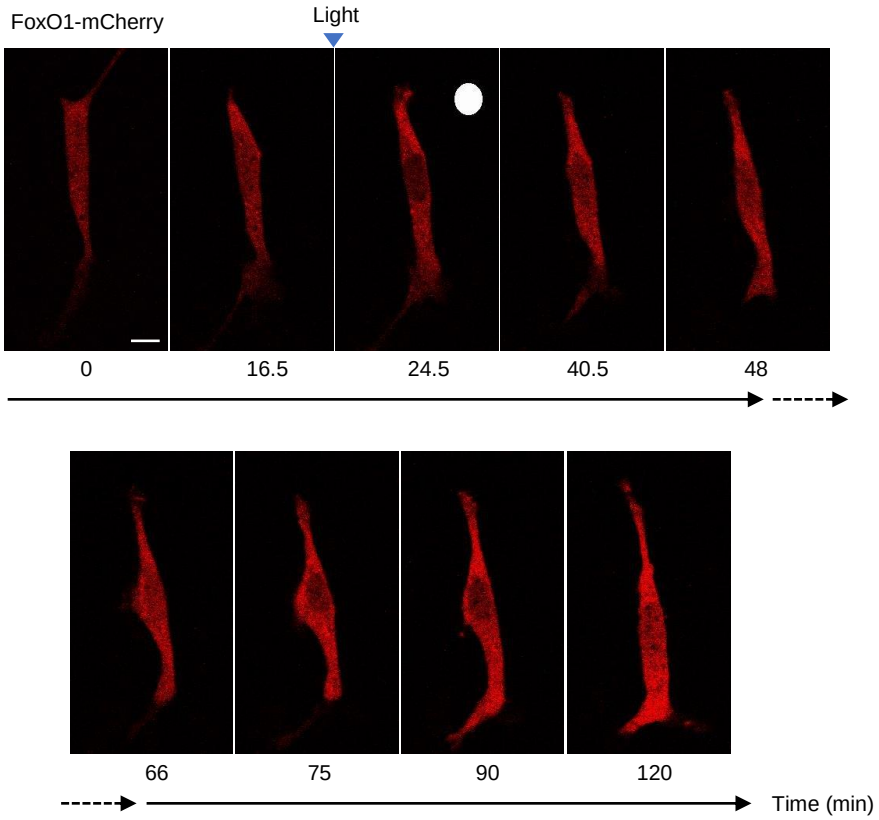

Figure 3-11. Oscillation of FoxO1 nuclear abundance.
C2C12 cell expressing Myr-CIBN, CRY2-Akt, and FoxO1-mCherry was illuminated with light pulses during 18–25 min time-point. Secondary nuclear exclusion of the FoxO1-mCherry was observed around 75–90 min time-point. White circle in the image of 24.5 min time-point indicates the light illumination for CRY2-Akt activation. Scale bar: 10 μm.

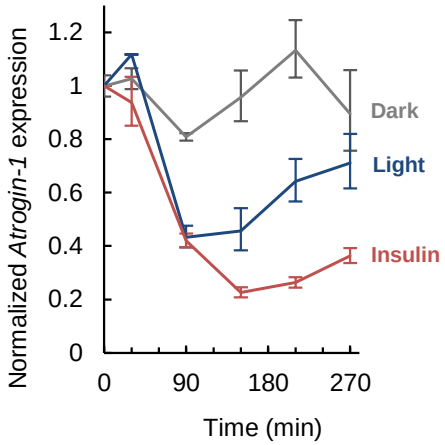

Figure 3-12. Optical control of FoxO1-regulated gene expression.
Light-induced down-regulation of FoxO1-regulated gene expression. Cells expressing Myr-CIBN and CRY2-Akt was continuously stimulated with 1 min interval of light pulses at 1 mW/cm^2 intensity.Bars: Mean±S.E.M. (*N*=4, biological replicates).

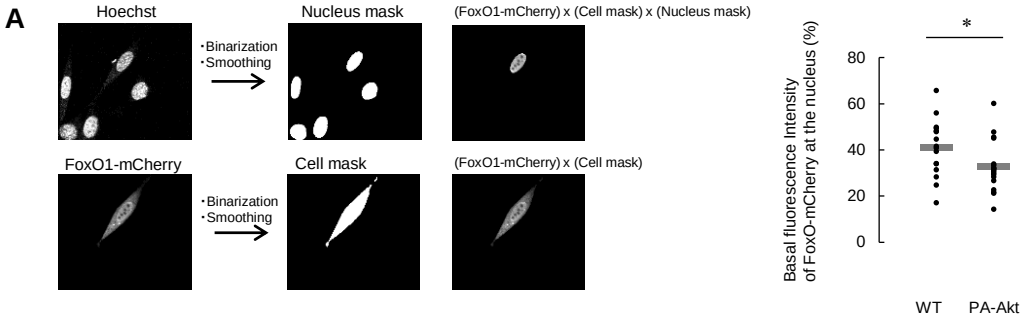

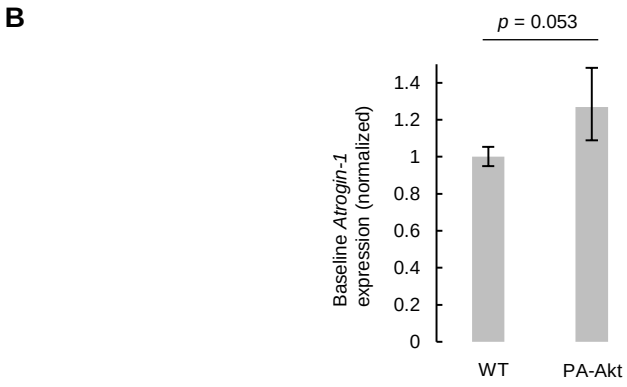

Figure 3-13. Baseline differences induced by the expression of Myr-CIBN and CRY2-Akt.
A. Basal activity of Myr-CIBN and CRY2-Akt to FoxO1-mCherry localization. The degree of nuclear localization of FoxO1-mCherry in the dark was quantified by using the cell and nucleus mask (*N*=15 for wild type C2C12 cells and *N*=19 for C2C12 cells expressing Myr-CIBN and CRY2-Akt). Cells were stained with a nuclear marker, Hoechst33342, and subsequently fixed with formaldehyde. **B.** Basal effect of Myr-CIBN and CRY2-Akt to *Atrogin-1* expression. *Atrogin-1* expression was measured with quantitative RT-PCR assays (*N*=4 for each condition).

3.3.2 Optical control of actin remodeling

Furthermore, to test the applicability of the developed system to perturb biological functions regulated by Akt, I investigated the effect of the activation of Akt signaling on actin remodeling. The results of previous studies suggested that Akt activity plays critical roles in reorganizing one of the cytoskeletal component protein, actin. Several target proteins including Rac-1[79], Girdin/APE[80,81], and Palladin[82] are proposed to link the signaling from Akt to actin reorganization, yet the detailed mechanisms of the Akt-mediated actin reorganization remain unknown[78,83]. Furthermore, several previous reports proposed an apparently contradictory result, negative contribution of Akt to actin reorganization[84,85], indicating the possibility that Akt changes its role depending on cellular contexts such as cell type and cell cycle.

Upon CRY2-Akt activation, a typical cellular morphological change, membrane ruffling formation, occurred in C2C12 cells (**Fig. 3-14A**). Moreover, a focal light stimulation perturbed cell polarity (**Fig. 3-14, B and C**), indicating that Akt activity is a driving force of actin reorganization at least in C2C12 cells. Taken together, these results demonstrate that the present PA-Akt system enables to control the dynamics of Akt activity, elucidating its functions in living cells.

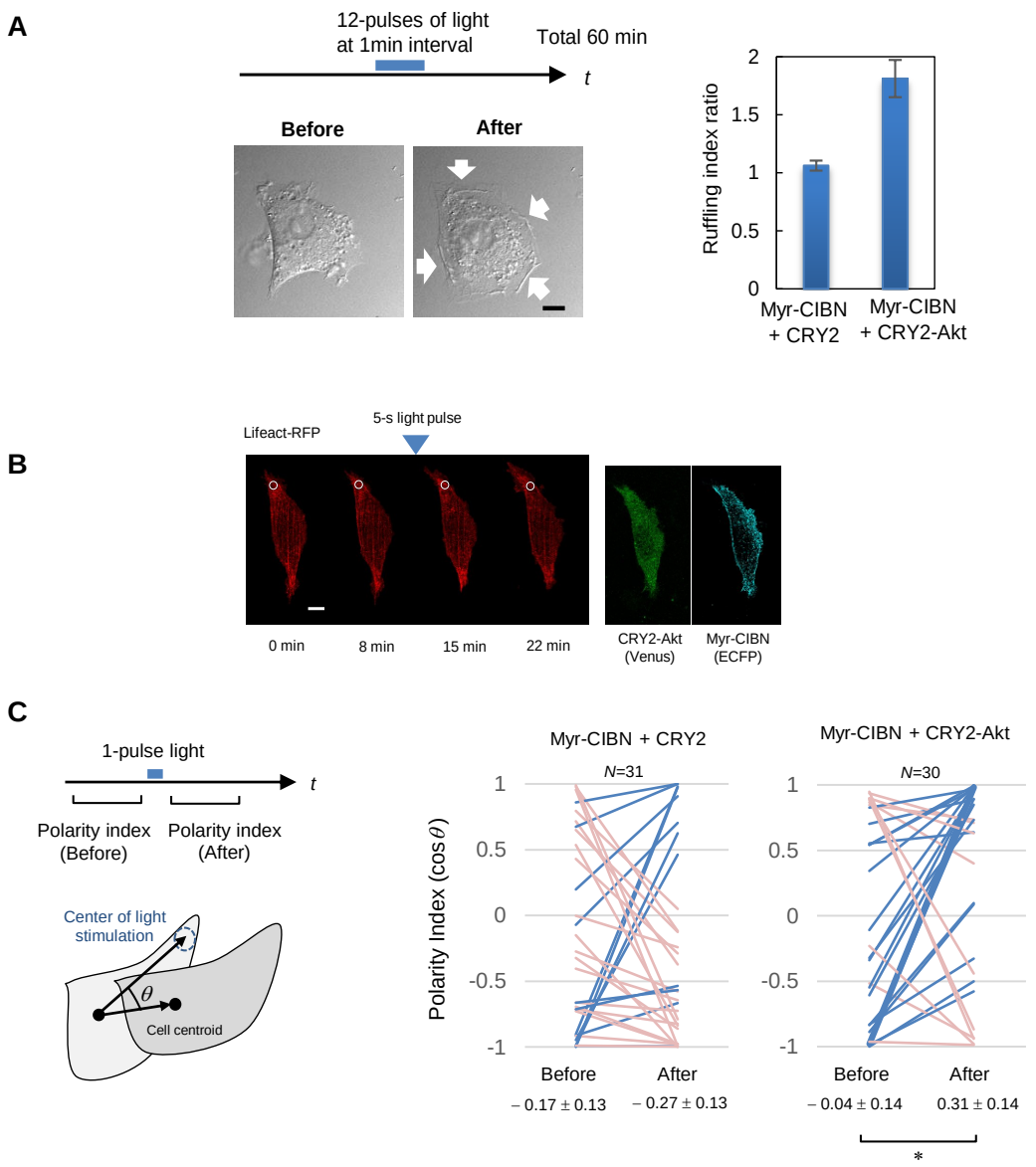

Figure 3-14. Optical control of Akt-induced actin remodeling.

A. Membrane ruffling formation induced by CRY2-Akt activation. (Left) Representative DIC images of the cell before and after 440-nm laser light stimulation. Arrows indicate the formation of membrane ruffling. Before image, 5 min before the first light pulse; After image, 13 min after the final light pulse; Scale bar, 10 μm. (Right) Changes of a membrane ruffling ratio induced by optical Akt activation. Bars: Mean±S.E.M. (*N*=25 for CRY2 control, *N*=29 for CRY2-Akt each in at least five independent experiments). **B.** Representative images of light-induced cell migration. Scale bar: 10 μm. Light-activation spot diameter: 5 μm. **C.** Statistical analysis of a light-induced cell migration by a focal Akt activation. Red lines indicate cells migrating to the light-illuminated spot while the blue lines indicate the cells migrating opposite direction from the light-illuminated spot (*N*=31 for control cells expressing Myr-CIBN and CRY2, *N*=30 for cells expressing Myr-CIBN and CRY2-Akt, * $p<0.05$ by a two-tailed paired *t*-test).

3.4 Discussion

I established an optical method to specifically perturb a protein kinase Akt activity with external light illumination. Upon light illumination, the kinase domain of Akt fused with a photoreceptor CRY2phr translocated to the cell membrane through light-induced hetero-dimer formation with a CRY2phr-interating partner protein, CIBN that was anchored at the plasma membrane. In principle, by replacing the CRY2phr-fused Akt isoform, the technique can be easily extended to other isoforms of Akt (Akt2 and Akt3) in addition to Akt1 isoform used in this study.

Although a chemically inducible system based on an interaction between FKBP and FRB with a dimerization-inducing cofactor rapamycin was previously developed to achieve an artificial control of Akt activity[86], the present approach has several advantages; the reversibility of the system in the minute timescale and the functionality without exogenous cofactor addition. The functionality without exogenous cofactor is of particular importance especially for *in vivo* applications such as manipulation of Akt activity in living mice. In the case of chemical control, the low solubility and non-uniform distribution of the exogenously added compound in living animals often hamper the applicability of those systems to *in vivo* manipulations. More fundamentally, chemical compounds themselves have a possibility to perturb signaling pathways, as rapamycin perturbs Akt signaling by binding to endogenous protein mTOR[87]. The genetically-encodable feature of the present optical system resolves these limitations of existing Akt control system. Although the optical control of FKBP–FRB system with *caged* rapamycin was previously demonstrated[88], the technique is irreversible and requires cytotoxic UV-light irradiation. Because of the dynamic spatiotemporal Akt activity in the physiological context, the ability to control the activity with light illumination is crucially important to investigate the functional roles of Akt in living systems.

In the optical manipulation of FoxO1 activity with specific Akt activation experiment, I found the oscillatory dynamics of FoxO1 nuclear abundance, which has not been reported in any

other extracellular stimulations. The finding underlines the potential of the developed method to analyze kinetic parameters responsible to FoxO1 dynamics and to reveal the physiological importance of the oscillatory behavior, as demonstrated in NF-κB which has similar oscillatory dynamics induced by stimulation of a ligand, TNF-α.

Although the developed optical technique has a large potential to address important issues, there are several further improvements that should be tackled in future. To achieve the comparable level activity of the PA-Akt system to endogenous Akt and a constitutively active type of Akt (Myr-Akt), the expression level of CRY2-Akt was optimized in high level compared with those of endogenous Akt and Myr-Akt (see Akt column in Figure 3-6), indicating that the efficiency of phosphorylation is smaller in CRY2-Akt than in endogenous Akt and Myr-Akt. The difference might result from two reasons mainly. First is an artifact of phosphorylation by the synthetic modules of CRY2phr and CIBN, which have a relatively large molecular weight and a defined native association kinetics between CRY2phr and CIBN. Identification of the minimal protein structure for the hetero-dimerization could increase the phosphorylation efficiency. Also, tunability of the association kinetics should be achieved as demonstrated in other photoreceptors[89–92], because the defined kinetics of association might affect the phosphorylation efficiency of Akt. Second reason is a requirement of other factors besides membrane translocation of Akt. While it was reported that a protein kinase PAK serves as a scaffold for the interaction of Akt and its upstream kinase PDK1[93], the optical regularity in the present system is limited to Akt translocation.

Additionally, another important challenge of the developed system is the low predictability of the light-induced Akt activity output. It is unclear how the light should be illuminated to achieve desired activation patterns of Akt. To address the issue, a general approach using mathematical modeling of the optical module will be described in the Chapter 4 of this thesis.

3.5 Conclusion

In conclusion, I developed an optical system that enables to specifically control the dynamics of Akt activity in a minute timescale within the physiological dynamic range. The developed system was applied to optical manipulation of the biological functions of Akt, FoxO1-induced gene expression and actin reorganization. Although the spatiotemporal Akt activity was visualized in diverse biological processes and human diseases, the method to reconstitute Akt activity using light has not been established. Therefore, unlike previous methods such as chemical stimulation and FKBP–FRB system, the developed optical method has a large potential to elucidate unknown physiological functions of Akt in the context of living systems. Importantly, the basic concept of the optical control described here can be principally extended to other biomolecules by modulating both the targeting signal sequence fused with CIBN and the protein of interest fused with photo-receptor CRY2.

Chapter 4.
Predictive Control of Temporal Patterns of Akt Activity

4.1 General significance of the mathematical model construction

Optogenetics provides unique approaches to deepen the understanding of the living systems by perturbing specific biomolecules of interest in a spatiotemporal manner, as described in the previous chapters. It was applied to artificial manipulation of versatile biological targets such as neuronal circuit[44,45], GTPase activity[52], organelle transport[63], and epigenetic state[62], and provided detailed insight in those fundamental biological processes. However, an important challenge of optogenetic manipulation remains in a difficulty to quantitatively predict the light-induced output. Because of the complicated processing of light input inside the living systems, the patterns of light illumination protocol do not match to those of light-induced output (**Fig. 4-1**). Herein, to manipulate optical systems in a precise quantitative manner, I aimed to establish a mathematical modeling approach to identify the *function* that links light input and light-induced output.

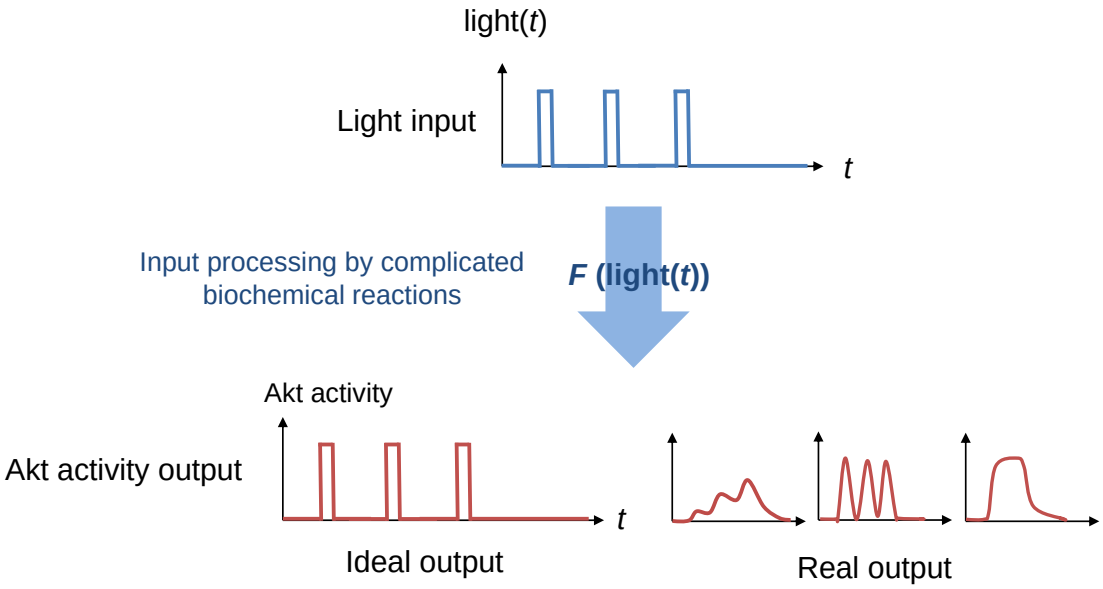

Figure 4-1. A difficulty in a precise predictive control of light-induced outputs.
Because of the complicated biochemical reactions (defined as *F*(light(*t*)) where light(*t*) is a protocol of light illumination with a function of time), the patterns of light illumination protocol do not match to those of light-induced output of optical modules.

4.2 Mathematical modeling of temporal patterns of CRY2-Akt activity

4.2.1 Non-feedback model

To precisely control the temporal patterns of CRY2-Akt activity with light input, I developed computational models and estimated their parameters using the experimentally obtained results of temporal CRY2-Akt activity patterns in cells stimulated with light pulses given at 1-min intervals under the optimized 4 mW/cm^2 light intensity condition (**Fig. 4-2A**). I first constructed an abstract model (Non-feedback model) in which cytosolic inactive CRY2-Akt was translocated to the plasma membrane upon light stimulation and was subsequently activated by upstream molecules (**Fig. 4-3**). However, the model with the set of estimated parameters was insufficient to predict the relative activation amplitude of CRY2-Akt (**Fig. 4-2B**), which was reproducible even at a different light intensity condition, 1 mW/cm^2 (**Fig. 4-4**). This result indicates that CRY2-Akt is non-linearly activated by an unknown mechanism of Akt activation.

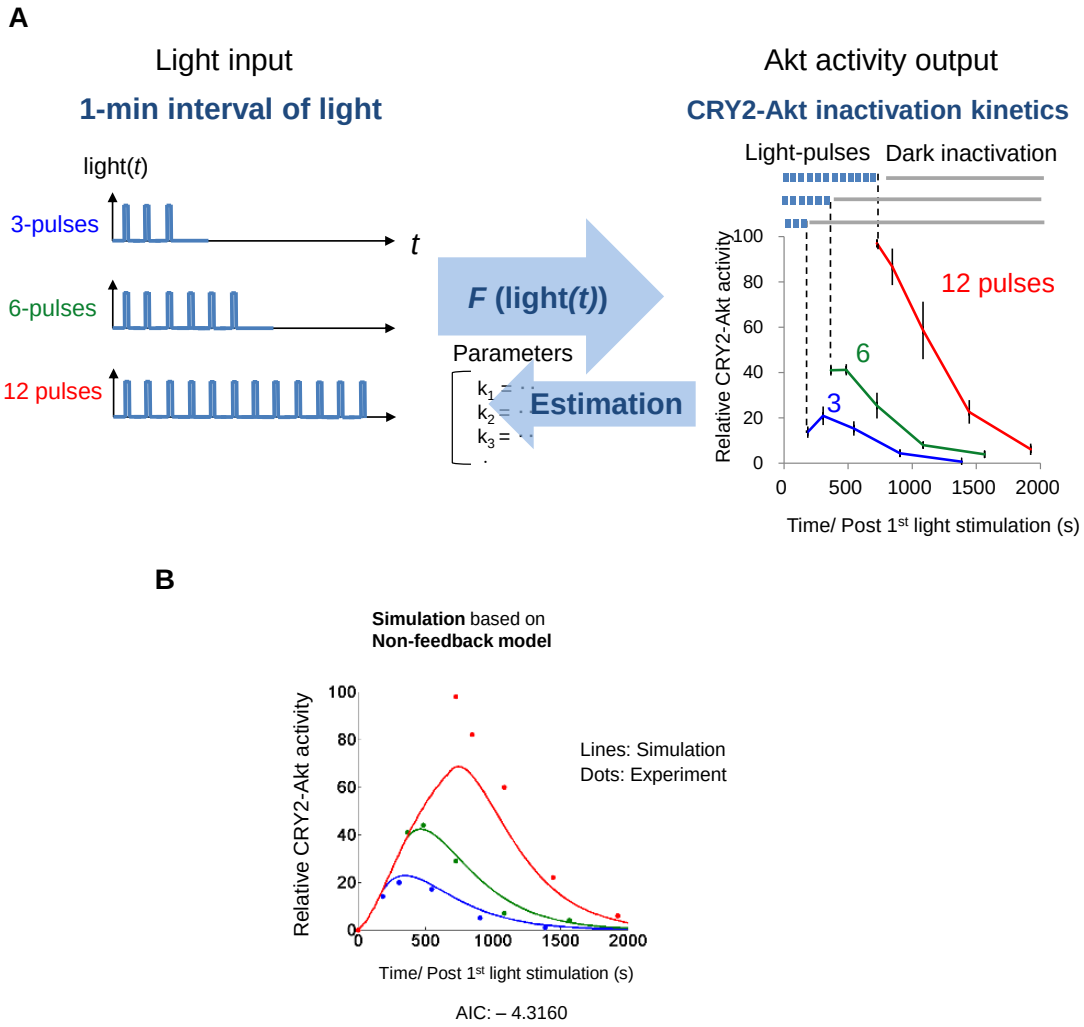

Figure 4-2. Time courses of CRY2-Akt activity.

A. C2C12 cells expressing Myr-CIBN and CRY2-Akt were stimulated 3, 6, or 12 times with light pulses at 1 min intervals. Relative CRY2-Akt activity was calculated by Western blot from Thr308 phosphorylation level of CRY2-Akt. Parameters in the model were estimated using the obtained data. The initiation of the first light pulse was set as time 0. Bars: Mean±S.E.M. (*N*=4, each in independent experiments). **B.** Simulations of CRY2-Akt activation based on Non-feedback model. The graph shows the time courses of CRY2-Akt activity in simulation (lines) and experiments (dots). A lower AIC value stands for a better fit.

A

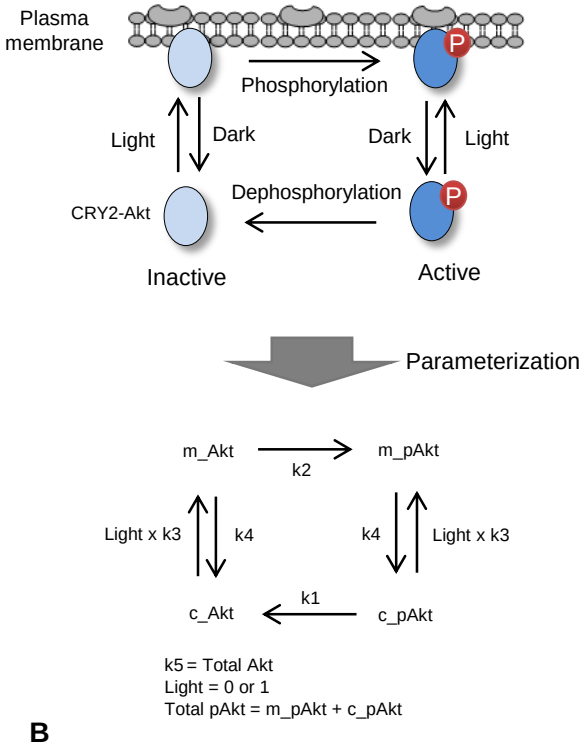

B

	Reaction	Reaction constant (/sec)	PN
A	c_pAkt → c_Akt	2.7903×10^{-3}	k1
B	mAkt → m_pAkt	4.7152×10^{-3}	k2
C	m_pAkt ⇄ c_pAkt	5.3363×10^{-3}, 3.5866×10^{-3}	k3,k4
D	m_Akt ⇄ c_Akt	5.3363×10^{-3}, 3.5866×10^{-3}	k3,k4

C

Initial amounts

Molecular name	Initial amounts	Parameter
c_pAkt	0	–
m_pAkt	0	–
c_Akt	1.0000×10^{3}	k5
m_Akt	0	–

D

ODEs

Differential equation	Re
$\frac{d[c\_pAkt]}{dt} = -k1 \cdot [c\_pAkt]$	A
$+ Light \cdot k3 \cdot [m\_pAkt]$	C
$- k4 \cdot [c\_pAkt]$	C
$\frac{d[m\_pAkt]}{dt} = k2 \cdot [m\_Akt]$	B
$- Light \cdot k3 \cdot [m\_pAkt]$	C
$+ k4 \cdot [c\_pAkt]$	C
$\frac{d[c\_Akt]}{dt} = k1 \cdot [c\_pAkt]$	A
$- Light \cdot k3 \cdot [c\_Akt]$	D
$+ k4 \cdot [m\_Akt]$	D
$\frac{d[m\_Akt]}{dt} = -k2 \cdot [m\_Akt]$	B
$+ Light \cdot k3 \cdot [c\_Akt]$	D
$- k4 \cdot [m\_Akt]$	D

Figure 4-3. Computational model of non-feedback CRY2-Akt activation.
A. Schematic of the non-feedback model: m_Akt, non-phosphorylated CRY2-Akt at membrane; c_Akt, non-phosphorylated CRY2-Akt at cytosol; m_pAkt, phosphorylated CRY2-Akt at membrane; c_pAkt, phosphorylated CRY2-Akt at cytosol. **B.** Reactions and rate constants in the model. PN: Parameter number. **C.** Initial amounts of molecules in the model. **D.** Ordinary differential equations (ODEs) in the model. Simulations were performed using Matlab (See also **Chapter 2.**).

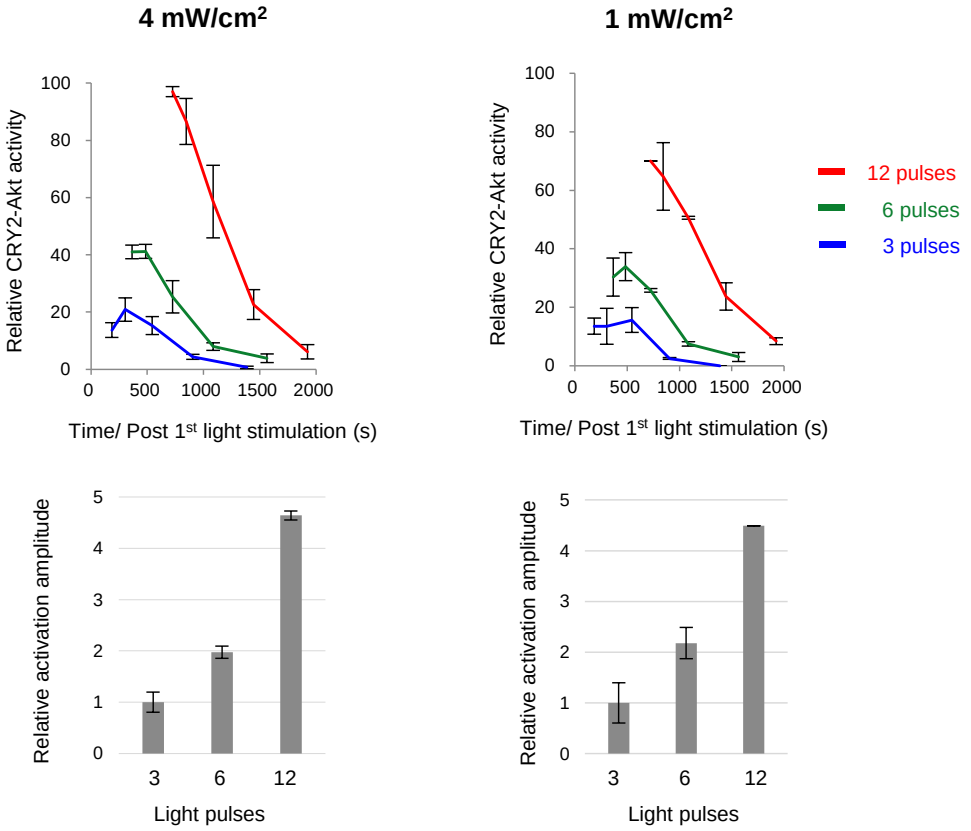

Figure 4-4. Light intensity dependency in the relative activation amplitude of CRY2-Akt. Almost the same relative activation amplitude was detected between 1 mW/cm^2 and 4 mW/cm^2 intensity of light. In the upper time course graphs, each CRY2-Akt amplitude was shown in relative to the amplitude of 1 min post 12 light pulses at 4 mW/cm^2 intensity condition. In the lower bar graphs, the relative activation amplitude between different numbers of light pulses was calculated from the highest CRY2-Akt activity in each time course. Bars: Mean±S.E.M. (*N*=4, each in independent experiment).

4.2.2 Feedback model

A positive feedback loop is one of the most fundamental network structures in intracellular signaling including PI3K signaling that may account for the nonlinear activation of Akt[94,95]. Based on such knowledge, feedback activation mode was incorporated into the model of Akt activation (Feedback model) (**Fig. 4-6**). Results showed that the simulation of a positive feedback activation model reproduced both the temporal patterns and the amplitude of Akt activity (**Fig. 4-5**). The model reproducibility was estimated using the Akaike Information Criterion (AIC)[69], which is a general measure of the relative goodness of fitted models. The AIC of the Feedback model was smaller than that of the Non-feedback model (**Fig. 4-7**), demonstrating that the fitting with the Feedback model is more reliable than that with the Non-feedback model. As AIC includes a penalty for the number of free parameters, the improved fitting is not simply derived from increased parameters.

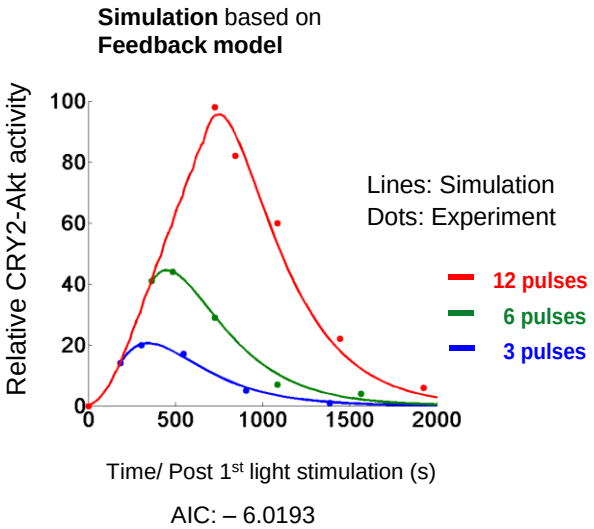

Figure 4-5. Simulations of the time courses of CRY2-Akt activity.
Simulations of CRY2-Akt activation based on Feedback model. The graph shows the time courses of CRY2-Akt activity in simulation (lines) and experiments (dots). A lower AIC value stands for a better fit.

A

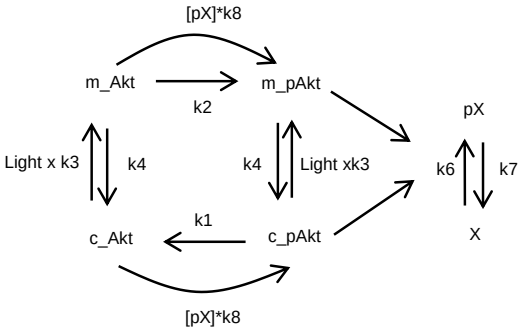

k5 = Total Akt
k9= Total X
Light = 0 or 1
Total pAkt = m_pAkt + c_pAkt

B

	Reaction	Reaction constant (/sec)	Parameter
A	c_pAkt → c_Akt	3.1300x 10^{-5}	k1
B	mAkt → m_pAkt	3.4503x 10^{-3}	k2
C	m_pAkt ⇄ c_pAkt	4.8355x 10^{1}, 7.0148x 10^{-3}	k3,k4
D	m_Akt ⇄ c_Akt	4.8355x 10^{1}, 7.0148x 10^{-3}	k3,k4
E	pX ⇄ X	4.6710x 10^{-2}, 5.5892x 10^{-1}	k6,k7
F	m_Akt + pX → m_pAkt + pX	4.1519x 10^{-4}	k8
G	c_Akt + pX → c_pAkt + pX	4.1519x 10^{-4}	k8

C

Initial amounts

Molecular name	Initial amounts	Parameter
c_pAkt	0	–
m_pAkt	0	–
c_Akt	8.9873x 10^{2}	k5
m_Akt	0	–
pX	0	–
X	6.7211x 10^{-1}	k9

D

ODEs

Differential equation	Reaction
$\frac{d[c\_pAkt]}{dt} = -k1 \cdot [c\_pAkt]$	A
$- Light \cdot k3 \cdot [m\_pAkt]$	C
$+ k4 \cdot [c\_pAkt]$	C
$+ k8 \cdot [c\_Akt] \cdot [pX]$	G
$\frac{d[m\_pAkt]}{dt} = k2 \cdot [m\_Akt]$	B
$+ Light \cdot k3 \cdot [m\_pAkt]$	C
$- k4 \cdot [c\_pAkt]$	C
$+ k8 \cdot [m\_Akt] \cdot [pX]$	F
$\frac{d[c\_Akt]}{dt} = k1 \cdot [c\_pAkt]$	A
$- Light \cdot k3 \cdot [c\_Akt]$	D
$+ k4 \cdot [m\_Akt]$	D
$\frac{d[m\_Akt]}{dt} = -k2 \cdot [m\_Akt]$	B
$+ Light \cdot k3 \cdot [c\_Akt]$	D
$- k4 \cdot [m\_Akt]$	D
$\frac{d[pX]}{dt} = k6 \cdot [X] \cdot ([m\_pAkt]+[c\_pAkt])$	F, G
$- k7 \cdot [pX]$	E

Figure 4-6. Computational model of feedback-mediated CRY2-Akt activation.
A. Schematic of the Feedback model: m_Akt, non-phosphorylated CRY2-Akt at membrane; c_Akt, non-phosphorylated CRY2-Akt at cytosol; m_pAkt, phosphorylated CRY2-Akt at membrane; c_pAkt, phosphorylated CRY2-Akt at cytosol. **B.** Reactions and rate constants in the model. PN: Parameter number. **C.** Initial amounts of molecules in the model. **D.** Ordinary differential equations (ODEs) in the model. Simulations were performed using Matlab (See also **Chapter 2.**).

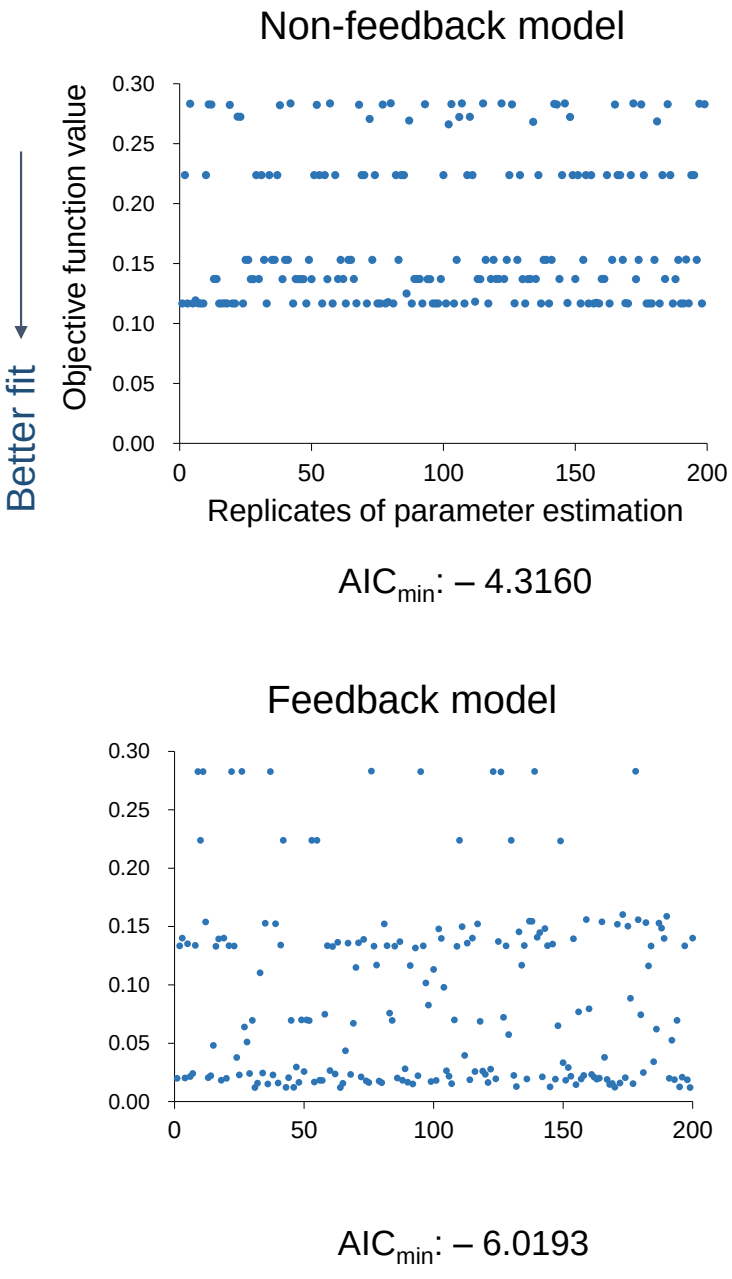

Figure 4-7. Summary of O.F.V. of parameter estimations with Non-feedback model (Upper) and with Feedback model (Lower).

4.3 Validation of the developed model and estimated parameters

4.3.1 Experimental confirmation of the feedback-mediated Akt activation

To confirm the network structure of the positive feedback loop experimentally, endogenous Akt phosphorylation was examined using the optical CRY2-Akt activation (**Fig. 4-8A**). The phosphorylation of endogenous Akt increased upon CRY2-Akt activation under a PTEN-phosphatase-inhibited condition (**Fig. 4-8B**). This endogenous Akt phosphorylation indicates the elevation of PIP3 amount: the existence of the positive feedback loop from Akt to its upstream activator PI3K, of which the activity is attenuated with PTEN. Because CRY2phr-fused Akt does not contain its PH domain in the optimized construct, the endogenous Akt activation implies the presence of elevated activity of upstream kinases of Akt, such as PDK1 and mTORC2; however the increased endogenous Akt phosphorylation was also detected in cells expressing Myr-CIBN and CRY2phr fused with a full-length of Akt (**Fig. 4-9**). The light-induced PIP3 production was also confirmed by a single molecule imaging of a PIP3 reporter, Akt labeled with a tetramethylrhodamine (TMR), under a total internal reflection fluorescence microscope (TIRFM) (**Fig. 4-10, A and B**). The number of detected PIP3 reporters at the plasma membrane increased upon CRY2-Akt activation, which was consistent with the increased endogenous Akt phosphorylation.

Furthermore, to investigate the mechanism of the feedback loop, I tested the inhibition influence of several probable components in the feedback loop. Actin polymerization, which has been demonstrated to be perturbed by Akt (**Fig. 3-14, A–C**), is known to function as a driving force of cellular events including feedback loops[96]. Results showed that the inhibition of the actin polymerization with Latrunculin B (Lat.B) suppressed the positive feedback loop completely (**Fig. 4-11A**). Suppression of endogenous Akt activity with Lat.B was also confirmed in cells stimulated with insulin (**Fig. 4-11B**), as described previously in other cell lines[97]. Taken together, these data suggest that Akt is activated by the positive feedback loop mediated by PI3K

activation and actin polymerization.

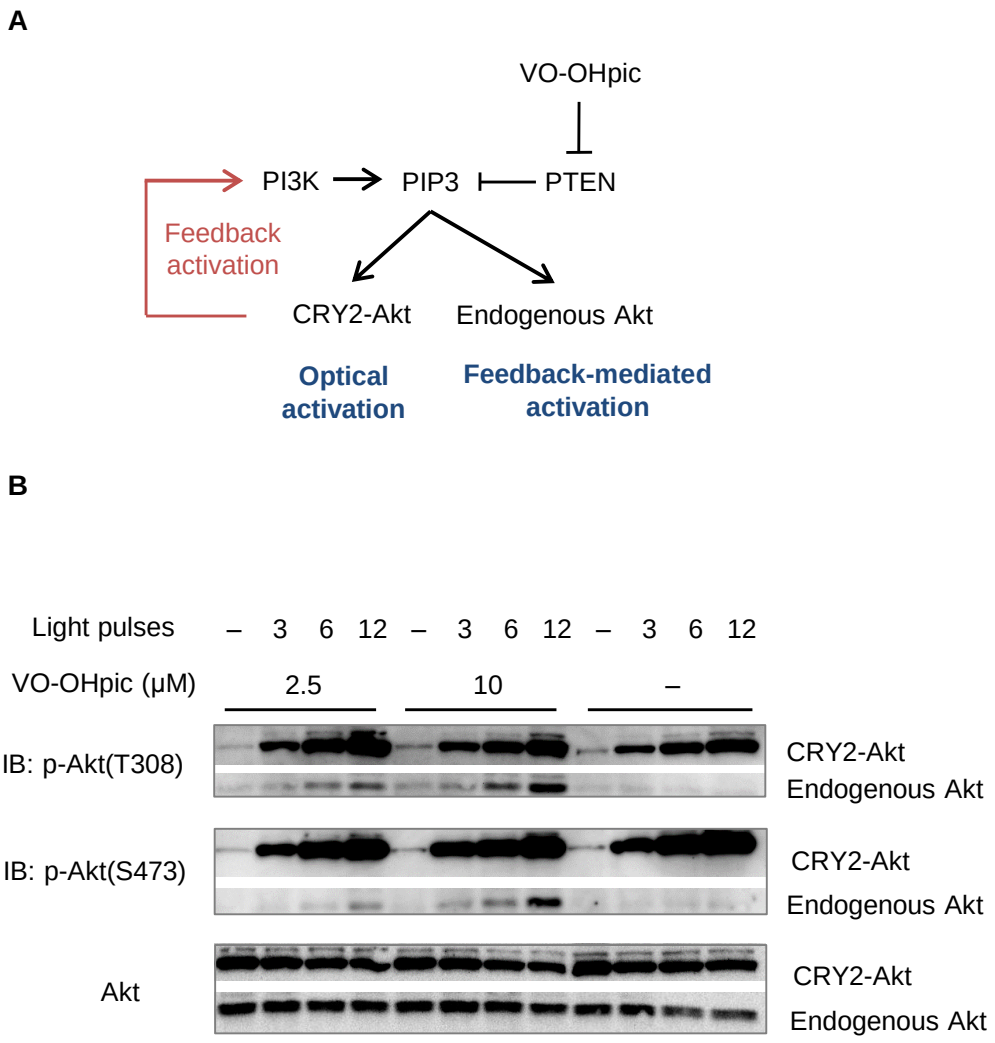

Figure 4-8. Experimental confirmation of feedback-mediated Akt activation.
A. Schematic of feedback-mediated PIP3 production by PI3K and the hydrolysis by PTEN.
B. Effects of PTEN inhibition on the activation of CRY2-Akt and endogenous Akt. C2C12 cells expressing Myr-CIBN and CRY2-Akt were pretreated with PTEN inhibitor, VO-OHpic for 15 min, and subsequently stimulated with 12 times of light pulses at 1 min interval.

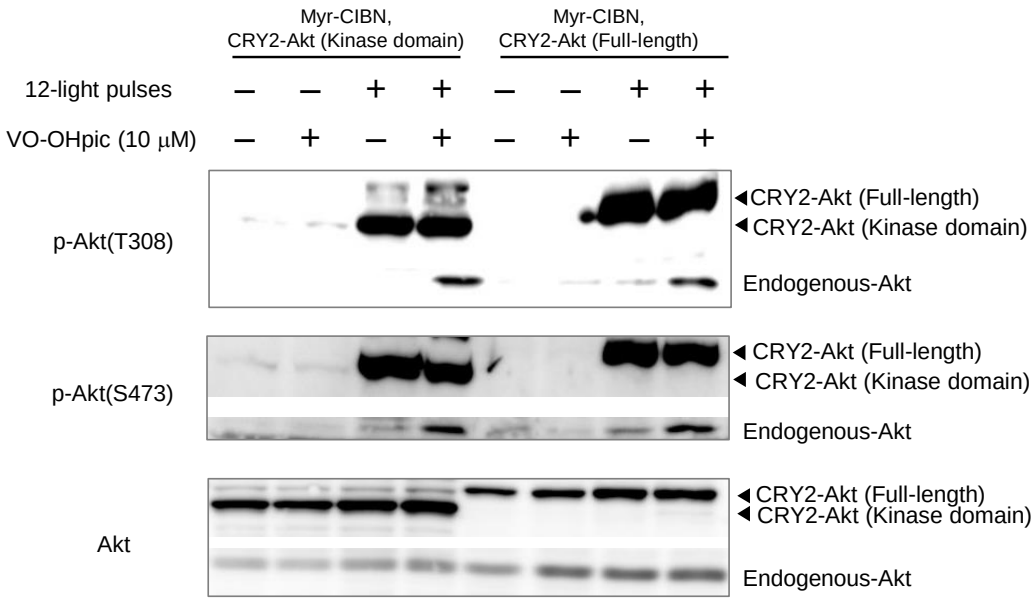

Figure 4-9. Full-length of PA-Akt.

Related to Figure 4-8B, phosphorylation of endogenous Akt was examined upon activation of CRY2-Akt(Full-length). C2C12 cells expressing Myr-CIBN and CRY2-Akt(Kinase domain) or CRY2-Akt(Full-length) were pretreated with PTEN inhibitor, VO-OHpic for 15 min, and subsequently stimulated with 12 times of light pulses at 1 min interval.

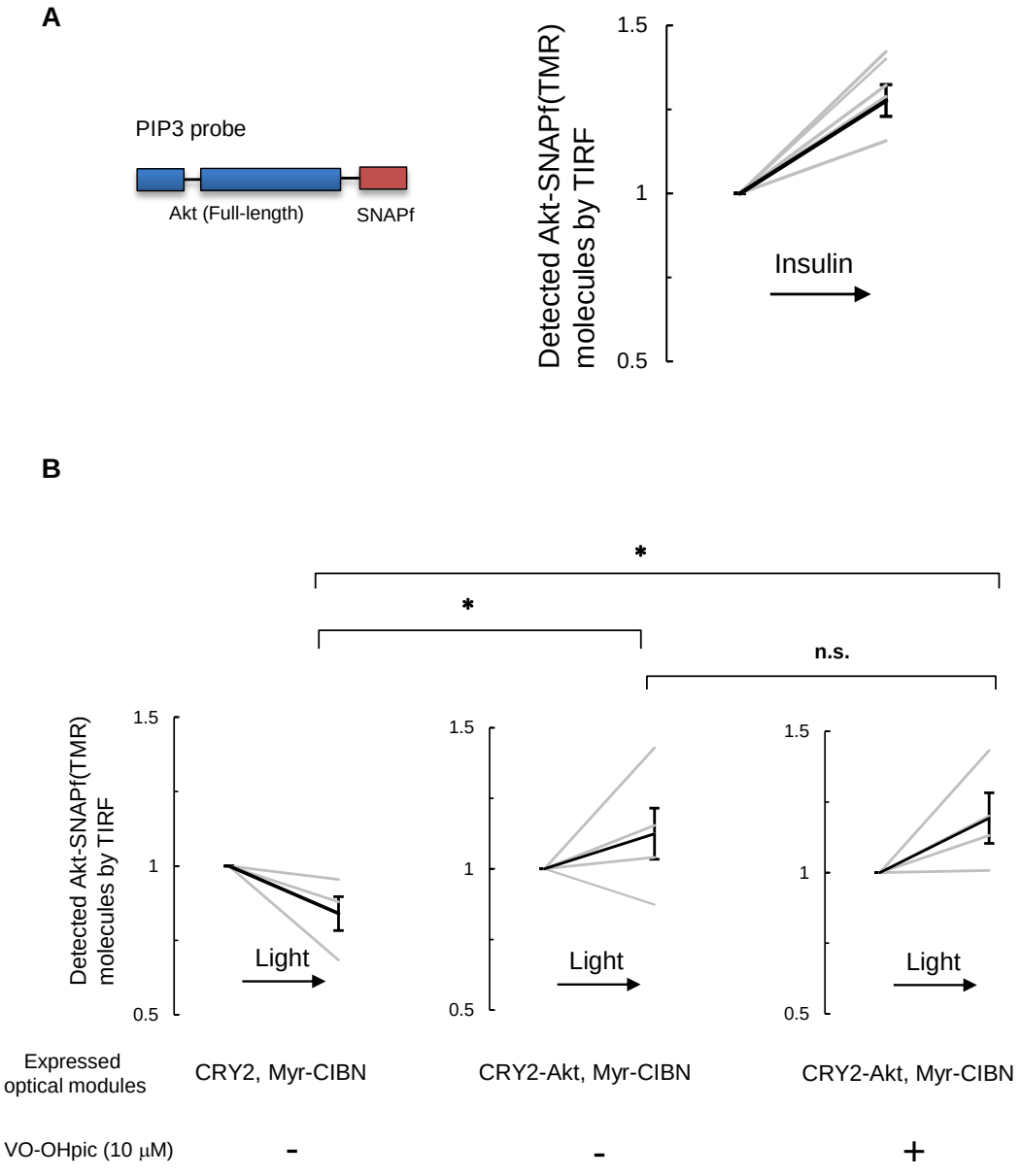

Figure 4-10. Light-induced PIP3 production observed by TRIFM.
A. Schematic of feedback-mediated PIP3 production by PI3K and the hydrolysis by PTEN. **B.** Effects of PTEN inhibition on the activation of CRY2-Akt and endogenous Akt. C2C12 cells expressing Myr-CIBN and CRY2-Akt were pretreated with PTEN inhibitor, VO-OHpic for 15 min, and subsequently stimulated with 12 times of light pulses at 1 min interval.

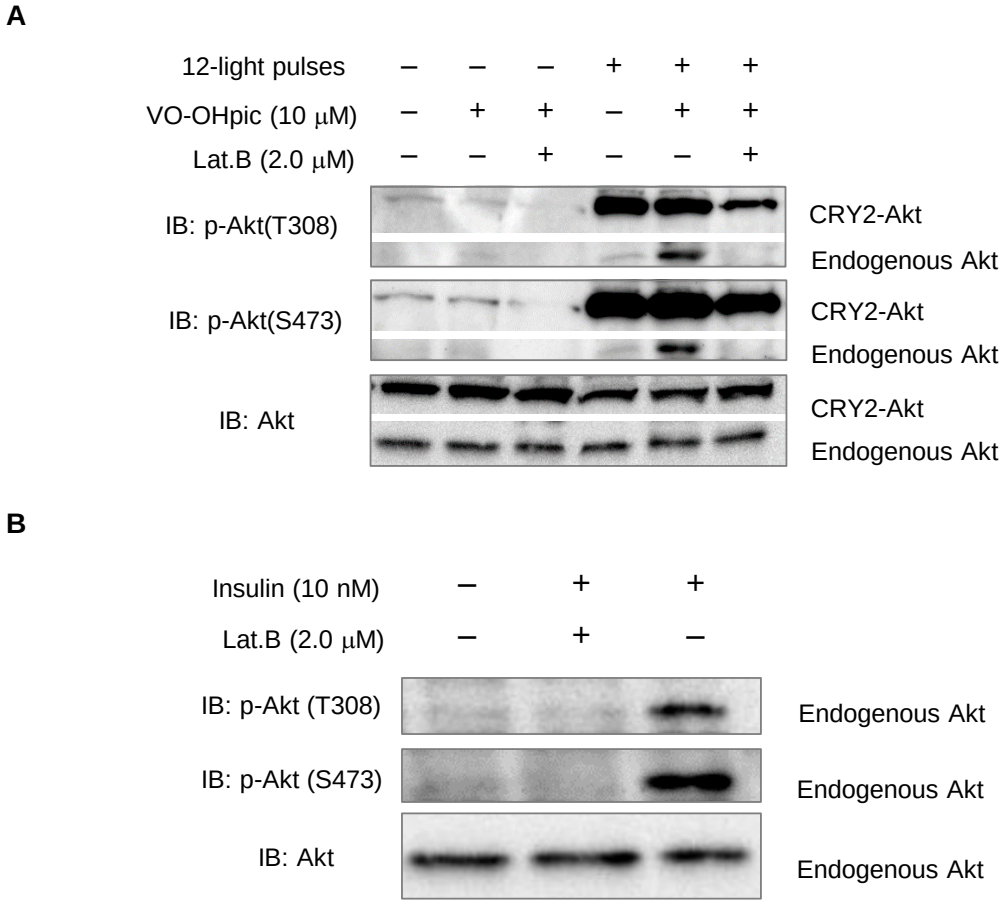

Figure 4-11. Inhibition of the positive feedback by Lat.B.
A. Inhibition of the positive feedback loop by an actin polymerization inhibitor, LatrunculinB (Lat.B). Cells expressing Myr-CIBN and CRY2-Akt were pretreated with 2 μM Lat.B and 10 μM VO-OHpic for 15 min, and were subsequently stimulated 12 times at 1 min intervals with light pulses. **B.** Inhibition of insulin-induced endogenous Akt activation by Lat.B. Serum-starved C2C12 cells were treated with insulin (10 nM) and Lat.B (2.0 μM) for 15 min and subjected to Western blot.

4.3.2 Qualitative validation of the developed model

To qualitatively test the ability of the Feedback model to predict experimentally obtained results, I examined CRY2-Akt activity under genetic and pharmacological perturbations (**Fig. 4-12**). PI3K inhibitors LY294002 and Wortmannin strongly attenuated the activation of CRY2-Akt (**Fig. 4-13**). These experimental features were reproduced by decreasing the rate constant of the parameter corresponding to PIP3 synthesis (k_6 in Figure 4-6). Additionally, I investigated the effects of genetic perturbations on CRY2-Akt activity. Overexpression of wild-type PTEN attenuated the activation of CRY2-Akt (**Fig. 4-14A**). In contrast, the expression of dominant negative mutants, PTEN(C124S) and PTEN(R130Q), which are markers of tumorigenesis[98], elevated the activation of CRY2-Akt (**Fig. 4-14B**). These results were also reproduced using simulations with the Feedback model. Taken together, these results suggest that the model with the estimated parameters correctly reconstitutes the intracellular CRY2-Akt dynamics.

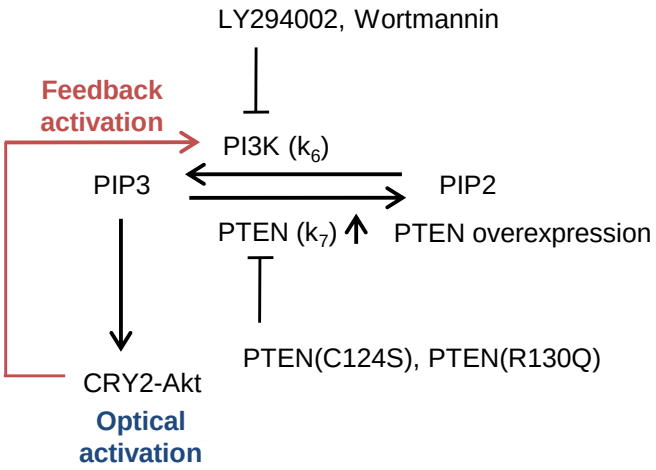

Figure 4-12. Schematic of genetic and pharmacological perturbations on CRY2-Akt.

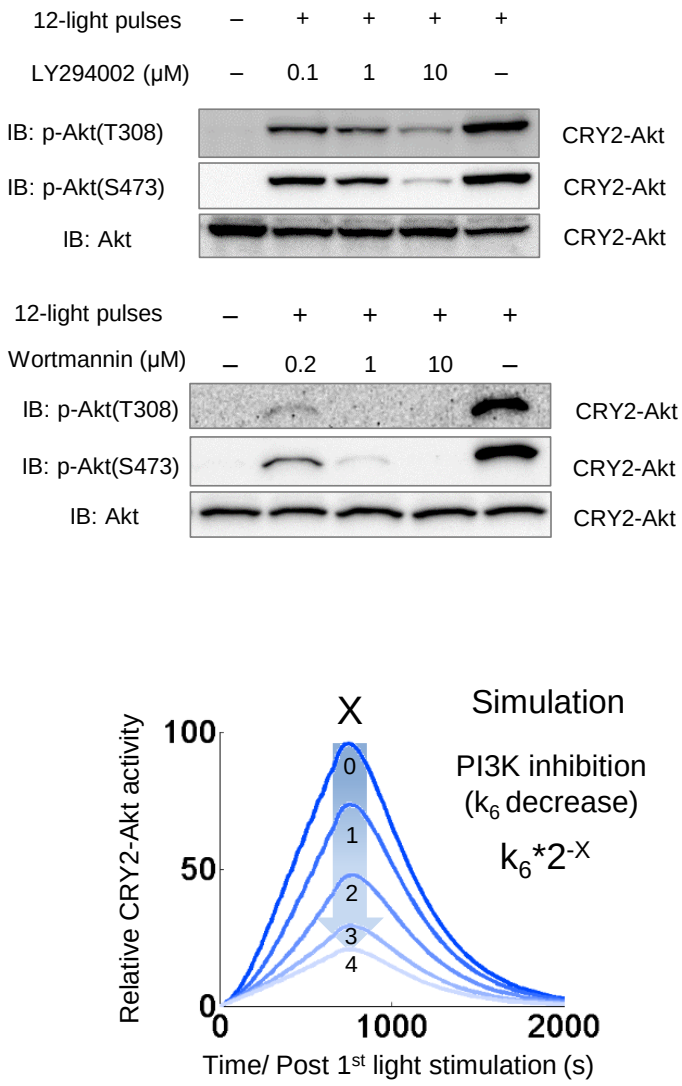

Figure 4-13. Effect of PI3K inhibition on the activation of CRY2-Akt.
C2C12 cells expressing Myr-CIBN and CRY2-Akt were pretreated with LY294002 (upper) or Wortmannin (middle) for 10 min and were subsequently stimulated 12 times with light pulses. (Lower) Simulations of PI3K inhibitor effect on CRY2-Akt activity. The amplitude of CRY2-Akt activation decreased by decreasing the rate constant of the parameter corresponding to PIP3 synthesis (k_6 in Figure 4-6). The initiation of the first light pulse was set as time 0.

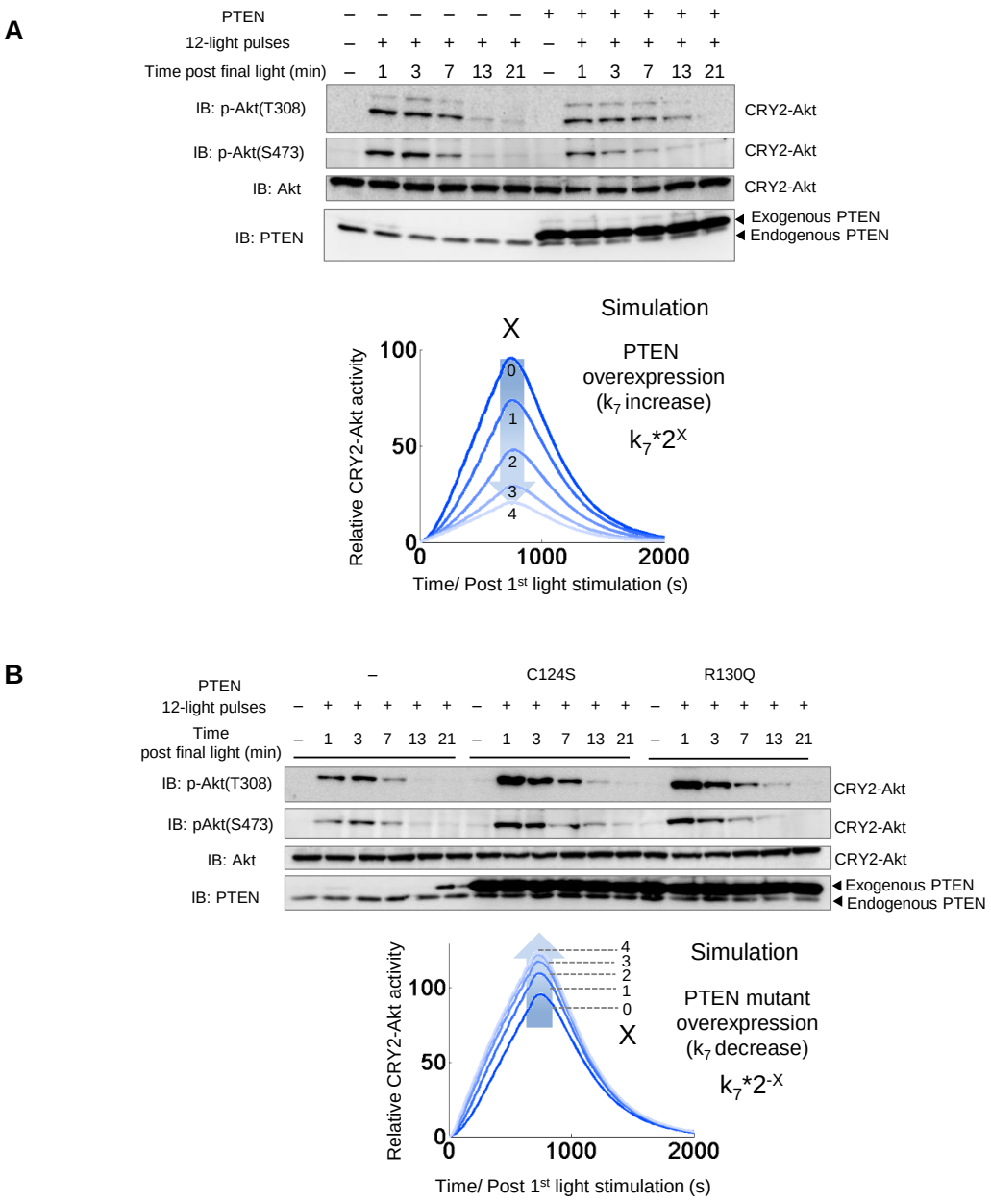

Figure 4-14. Genetic perturbations on CRY2-Akt.

A. (Left) Effect of PTEN overexpression on the CRY2-Akt activity. C2C12 cells expressing Myr-CIBN, CRY2-Akt, and wild-type PTEN were stimulated 12 times with light pulses. (Right) Simulations of the effects of PTEN expression on the CRY2-Akt activity. The amplitude of CRY2-Akt activation decreased by increasing the rate constant of the parameter corresponding to PIP3 hydrolysis (denoted as k_7 in **Fig. 4-6**). **B.** (Upper) Effect of PTEN expression on the CRY2-Akt activity. C2C12 cells expressing Myr-CIBN, CRY2-Akt, and dominant negative PTEN mutants (PTEN(C124S), PTEN(R130Q)) were stimulated 12 times with light pulses. (Lower) Simulations of the effects of PTEN expression on the CRY2-Akt activity. The amplitude of CRY2-Akt activation increased by decreasing the rate constant of the parameter corresponding to PIP3 hydrolysis (denoted as k_7 in **Fig. 4-6**).

4.3.3 Quantitative validation of the developed model

Furthermore, to quantitatively test the model's predictability of experimental results, I performed a cross-validation assay using new datasets of temporal CRY2-Akt patterns, which were not used for parameter estimations. I examined temporal CRY2-Akt patterns in different light stimulation conditions (0.5-min, 3-min, and 5-min intervals). The PA-Akt system generated different temporal patterns of CRY2-Akt activity under each light stimulation condition. These patterns were well predicted by the simulations based on the Feedback model, but not by the simulations based on the Non-feedback model (**Fig. 4-15**). Specifically, simulations based on the Feedback model predicted the lower activation amplitude of CRY2-Akt under the 0.5-min interval time condition better than the simulations based on the Non-feedback model, indicating that CRY2-Akt was activated with feedback-mediated increasing speed. Consequently, I concluded that the Feedback model enabled the predictive control of the temporal patterns of CRY2-Akt activity even under different light stimulation conditions and genetic and pharmacological perturbations.

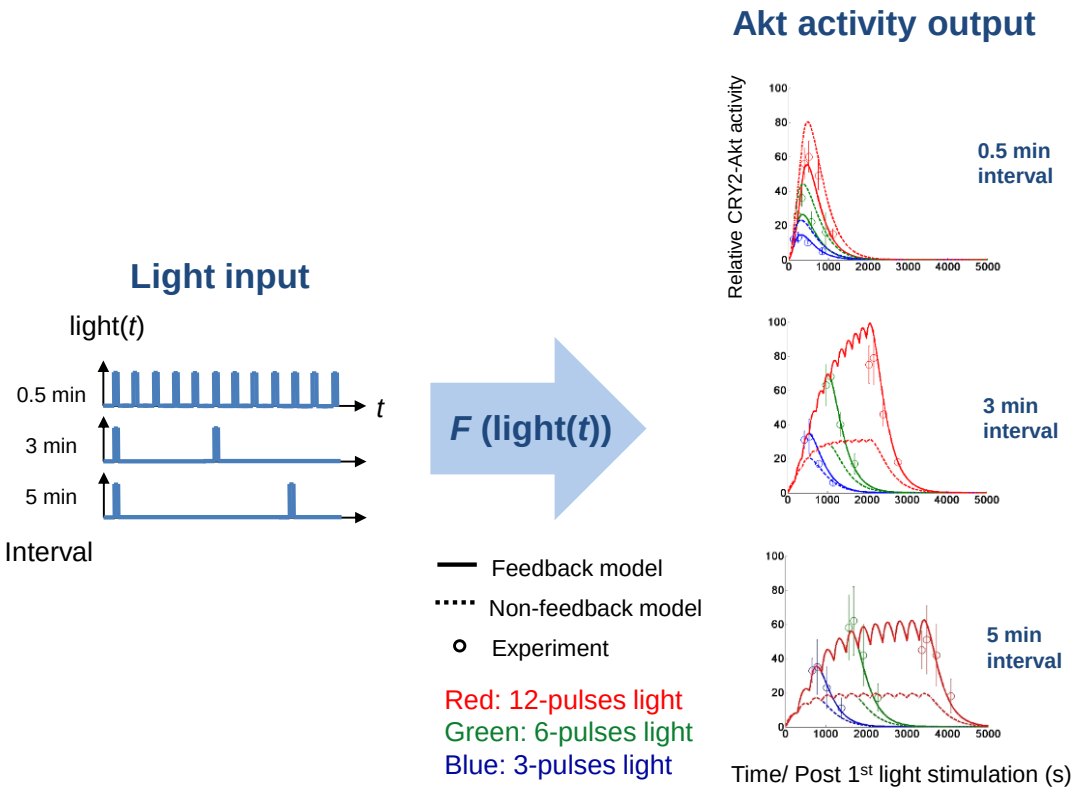

Figure 4-15. Quantitative validation of the developed mathematical model.
C2C12 cells expressing Myr-CIBN and CRY2-Akt were stimulated with different intervals of light, 0.5-min, 3-min, and 5-min interval. Circles show the relative CRY2-Akt activity evaluated from the Thr308 phosphorylation. Lines and dotted lines respectively show simulations by the Feedback model and the Non-feedback model. Bars: Mean±S.E.M. (*N*=4, each in independent experiments).

4.4 Functional analysis of the temporal patterns of Akt activity

Finally, to demonstrate the utility of the developed system with computational model, I investigated the cellular response with different temporal patterns of Akt activity. The cells were stimulated with three different patterns of Akt activity (Light-12, Light-6, and Light-3) as an input using custom-built LED array. *Atrogin-1* expression was measured as a cellular output. The total active CRY2-Akt dose was set to the equal amount between different patterns of stimulations based on the mathematical model simulations. Intriguingly, *Atrogin-1* expression decreased under Light-3 and Light-6 conditions but not Light-12, which produced a higher amplitude and lower frequency of Akt activity (**Fig. 4-16**). This result strongly suggests that cells have a mechanism by which specific temporal patterns of Akt activity are captured as an informative cellular input.

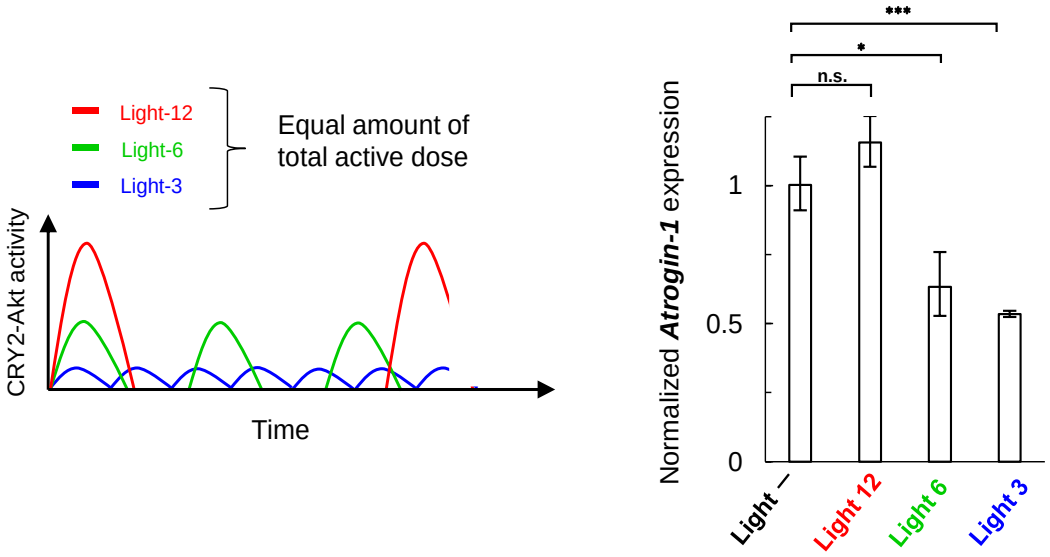

Figure 4-16. Functional analysis of temporal Akt activity.
Each of the CRY2-Akt activation pattern was generated by illuminating cells with 1-min interval of light pulses at 1 mW/cm^2 intensity. *Atrogin-1* expression was measured at a time point of 200 min after the onset of light illumination. Activation interval: 16.0 min (Light-3), 36.5 min (Light-6), 91.0 min (Light-12). Last light pulse was added 6.0 min (Light-3), 12.5 min (Light-6), and 7.0 min (Light-12) before the collection of cells. *p < 0.05, ***p < 0.001 by a two-tailed Student's t-test. n.s.: not significant. Bars: Mean±S.E.M. (N=3)

4.5 Discussion

I described a mathematical model-based approach to precisely control the temporal activity patterns of the developed optical module CRY2-Akt. The mathematical model with estimated parameters correctly reproduced the experimentally obtained results with western blotting assays. The ability to reconstitute the temporal Akt dynamics at will with the mathematical model and the custom-built LED array system enabled to elucidate the functional significance of temporal Akt dynamics, which has not been investigated because of the lack of an ideal method to analyze it. I demonstrated that the temporal patterns of Akt are pivotal in inducing its downstream biological function, *Atrogin-1* expression. The methodology described here will facilitate the elucidation of general signal processing mechanism of Akt and its biological significance.

Although the approach with the model-based predictive control would provide an important advance in the optogenetic control of Akt, there are several limitations at present. First, the model is not directly applicable to the CRY2-Akt dynamics induced by other stimulations such as extracellular growth factors, because our model currently assumes only the contribution of light to CRY2-Akt dynamics. For instance, insulin stimulation activates several signaling pathways simultaneously in addition to Akt, which probably affects the temporal dynamics of CRY2-Akt. For the same reason, the precision of model prediction may sometimes be inaccurate when the system is used in a condition where other factors that perturb CRY2-Akt dynamics exist, such as under an *in vivo* condition. Second, the simulation did not fully match the experimental data when the cells were illuminated with intervals of light other than 1-min. This discrepancy may originate from errors in the experimental data used for parameter estimations owing to the difficulty of precisely quantifying phosphorylated Akt in western blotting assays. The development of more precise quantification methods will strengthen the present system in terms of model prediction.

In an attempt to construct a computational model of temporal Akt dynamics, I found that Akt uses a positive feedback activation mode, which is mediated by PI3K activation and actin polymerization. In accordance with previous studies[80,83,99,100], I found that optical activation of Akt is sufficient to perturb cellular polarity, supporting the existence of the positive feedback activation mode, because it is known that feedback networks play a key role in generating spatially and temporally confined signals to break a symmetry[94,95]. I anticipate that the detailed mechanism of the actin-related feedback mechanism will be revealed by taking advantage of the developed optogenetic system to perturb the Akt activity in a single cell level.

While the predictability of the light-induced output is limited in the temporal dynamics at the present stage, the strategy of light-induced output prediction with computational modeling can be principally extended to the spatial dynamics by obtaining experimental data of spatial Akt dynamics with light illumination. Furthermore, the overall strategy described in this chapter is applicable to other optogenetic systems, offering a general framework to manipulate optogenetic tools in a precise quantitative manner.

4.6 Conclusion

In summary, I developed a mathematical model-based approach, which allows to control the temporal dynamics of the developed optogenetic Akt system in a precise predictive manner. The model with experimental data indicated that Akt is activated by the positive feedback loop through PI3K activation and actin polymerization. Because of the central roles of Akt in various biological processes and human diseases, the ability to control the activity precisely at the desired level is expected to facilitate versatile applications especially in therapeutic treatment and synthetic biology. The present approach of optogenetic output prediction with computational modeling will provide a general strategy to interrogate the functional significance of temporal dynamics of biomolecules.

Chapter 5.
General Conclusion

Akt or Protein Kinase B is one of the most important protein kinases that regulate diverse biological processes, such as glucose metabolism, cell differentiation, and protein synthesis. However, the precise control of its kinase activity remains to be achieved at the current stage, in spite of the huge need in life sciences and clinical treatments. To address the issue, I developed an optical approach (optogenetics) that has a potential to control the spatiotemporal dynamics of Akt activity. Furthermore, to overcome a general limitation in the field of optogenetics: the low-predictability of light-induced optogenetic output, I established a mathematical model-based approach by which the activity of the developed optogenetic Akt system was temporally controlled in a precise predictive manner.

In Chapter 3 of the thesis, I described the optogenetic approach to control the Akt activity using external light illumination. Upon light illumination, Akt fused with *Arabidopsis thaliana* photoreceptor CRY2phr was transiently localized at the cell membrane and subsequently activated, which was mediated by light-induced hetero-dimerization between CRY2phr and cell membrane-anchored CRY2phr-interating partner protein, CIBN. The activation was controlled in a minute timescale and optimized within the physiological dynamic range of Akt activity. The achieved system enabled to specifically control the biological functions of Akt, induction of cell polarity and suppression of the gene expression responsible for muscle atrophy. These results indicate the potential of the present method to facilitate the detailed elucidation of Akt functions in various contexts of live cells.

In Chapter 4, I introduced mathematical modeling to manipulate the optogenetic Akt system precisely in a quantitative manner. The constructed mathematical model, in which the newly-identified feedback activation mode of Akt was incorporated, correctly reproduced the light-induced temporal Akt dynamics even in the presence of the pharmacologic and genetic perturbations on Akt signaling pathways. Furthermore, taking advantage of the precise quantitative regularity of the Akt dynamics, I obtained the direct evidence that the temporal dynamics of Akt is functionally important to induce the downstream biological function of Akt.

The results clearly indicates that biological behavior should be investigated and linked with a spatiotemporal cellular context.

As a future perspective of this research, there would be mainly three promising advancement in future. First, the biological functions of temporal Akt activities would be revealed in a more comprehensive biological context instead of the specific target gene, *Atrogin-1*. The combination of the developed optical Akt tool with techniques such as DNA microarray and metabolomics that allow to obtain a large number of data on gene expression and metabolite would provide comprehensive biological functions of temporal Akt activity. Second, the general concept of constructing optical tools would be extended to other kinases and also to phosphatases, because those molecules' activities are controlled with a common mechanism, the protein–protein interaction. The development of a variety of optical tools allows to reveal specific functions of the target molecule and also it would provide a more general insight into the biological functions of temporal patterns of biomolecules. Third, the mathematical model-based quantitative control approach would be applied to other optogenetic systems, which currently lack the precise spatiotemporal regularity. The overall approach would allow to maximize the use of advantages derived from optogenetics.

Taken together, I established the optical approach to specifically control the Akt activity in a minute timescale within the physiological dynamic range of Akt activity. In combination with mathematical modeling-based approach, the optical system achieved the precise predictive control of temporal Akt activity. Importantly, the technique descried here is general, thereby widely applicable to developing other optogenetic systems with precise spatiotemporal regularity. The present approach has a potential to make a huge step forward to deepen our understating of the fundamentals in biological systems.

Acknowledgement

The present thesis was completed under the supervision of Prof. Takeaki Ozawa. I would like to express my sincere appreciations for his constant support, guidance, and encouragement to complete my research throughout the study. I appreciated all the stuff members in Prof. Ozawa lab., especially Dr. Akira Kanno, Dr. Hideaki Yoshimura, Dr. Mitsuru Hattori, and Dr. Hideo Takakura for a number of stimulating discussions and their critical comments on my research. Also, I have greatly benefited from well talented other graduate students in Prof. Ozawa lab., who gave a lot of intuitive suggestions and precious peer pressure. Without the environmental advantages, I would not maintain the high level of motivation for science, which enables me to work hard throughout my research.

The mathematical modeling part in Chapter 4 was heavily supported by Prof. Shinya Kuroda lab., especially by Prof. Hiroyuki Kubota and Dr. Katsuyuki Kunida. I had a great opportunity to learn systems biology, which, I believe, will become beneficial throughout my future carrier. I would like to express my sincere appreciations for their time devotion for helping me to construct mathematical models and for critically reading the manuscript. Without their kind supports, this thesis would not be completed.

I thanks Advanced Leading Graduate Course for Photon Science (ALPS) and JSPS Research Fellowship for Young Scientists for their financial supports and overseas experience. Especially in ALPS program, I deeply appreciated Prof. Michael White in the University of Manchester for hosting me in U.K. and Prof. Mitsuhiko Shionoya for his encouragement as a secondary supervisor throughout my Ph.D. course.

Finally, I gave great thanks to my family for giving me this great opportunity to study in the University of Tokyo and also for encouraging me to do what I truly love to do. I cherish all the priceless experiences in Prof. Ozawa lab. in the University of Tokyo.

References

1. Ubersax, J. A. & Ferrell, J. E. Mechanisms of specificity in protein phosphorylation. *Nat. Rev. Mol. Cell Biol.* **8,** 530–541 (2007).

2. Johnson, L. N. The regulation of protein phosphorylation. *Biochem. Soc. Trans.* **37,** 627–641 (2009).

3. Manning, G., Whyte, D. B., Martinez, R. & Hunter, T. The Protein Kinase Complement of the Human Genome. **870,** (2002).

4. Genomics, C. Finishing the euchromatic sequence of the human genome. 931–945 (2001).

5. Gonzalez, E. & McGraw, T. E. The Akt kinases: Isoform specificity in metabolism and cancer. *Cell Cycle* **8,** 2502–2508 (2009).

6. Gonzalez, E. & McGraw, T. E. Insulin-modulated Akt subcellular localization determines Akt isoform-specific signaling. *Proc. Natl. Acad. Sci. U. S. A.* **106,** 7004–9 (2009).

7. Wu, W. I. *et al.* Crystal structure of human AKT1 with an allosteric inhibitor reveals a new mode of kinase inhibition. *PLoS One* **5,** (2010).

8. Obata, T. *et al.* Peptide and protein library screening defines optimal substrate motifs for AKT/PKB. *J. Biol. Chem.* **275,** 36108–15 (2000).

9. Alessp, D. R., Caudwell, F. B., Andjelkovic, M., Hernmings, B. A. & Cohen, P. Molecular basis for the substrate specificity of protein kinase B ; comparison with MAPKAP kinase-1 and p70 S6 kinase. **399,** 333–338 (1996).

10. Manning, B. D. & Cantley, L. C. AKT/PKB signaling: navigating downstream. *Cell* **129,** 1261–74 (2007).

11. Hers, I., Vincent, E. E. & Tavaré, J. M. Akt signalling in health and disease. *Cell. Signal.* **23,** 1515–27 (2011).

12. Alessi, D. R. *et al.* Characterization of a 3-phosphoinositide-dependent protein kinase which phosphorylates and activates protein kinase Bα. *Curr. Biol.* **7,** 261–269 (1997).

13. Sarbassov, D. D., Guertin, D. A. & Ali, S. M. Phosphorylation and Regulation of Akt / PKB by the Rictor-mTOR Complex. *Science (80-.).* **307,** 1098–1102 (2005).

14. Sci, A. N. Y. A. *et al.* PTEN , a Putative Protein Tyrosine Phosphatase Gene Mutated in Human Brain , Breast , and Prostate Cancer. **275,** 1943–1948 (1997).

15. Andjelkovic, M., Jakubowicz, T., Cron, P., Ming, X. & Han, J. pleckstrin homology. **93,** 5699–5704 (1996).

16. Gao, T., Furnari, F. & Newton, A. C. PHLPP: a phosphatase that directly dephosphorylates Akt, promotes apoptosis, and suppresses tumor growth. *Mol. Cell* **18,** 13–24 (2005).

17. Lasserre, R. *et al.* Raft nanodomains contribute to Akt/PKB plasma membrane recruitment and activation. *Nat. Chem. Biol.* **4,** 538–47 (2008).

18. Yasukawa, T. *et al.* S-nitrosylation-dependent inactivation of Akt/protein kinase B in insulin resistance. *J. Biol. Chem.* **280,** 7511–8 (2005).

19. Carpten, J. D. *et al.* A transforming mutation in the pleckstrin homology domain of AKT1 in cancer. *Nature* **448,** 439–44 (2007).

20. Lindsay, J. R. *et al.* Meal-Induced 24-Hour Profile of Circulating Glycated Insulin in Type 2 Diabetic Subjects Measured by a Novel Radioimmunoassay. 631–635 (2003). doi:10.1053/meta.2003.50105

21. O'Rahilly, S., Turner, R. C. & Matthews, D. R. Impaired pulsatile secretion of insulin in relatives of patients with non-insulin-dependent diabetes. *N. Engl. J. Med.* **318,** 1225–30 (1988).

22. Kubota, H. *et al.* Temporal Coding of Insulin Action through Multiplexing of the AKT Pathway. *Mol. Cell* **46,** 820–832 (2012).

23. Noguchi, R. *et al.* The selective control of glycolysis, gluconeogenesis and glycogenesis by temporal insulin patterns. *Mol. Syst. Biol.* **9,** 664 (2013).

24. George, S. *et al.* A Family with Severe Insulin Resistance and Diabetes Due to a Mutation in AKT2. **304,** 1325–1329 (2004).

25. Bellacosa, A., Testa, J. R., Staal, S. P. & Tsichlis, P. N. A retroviral oncogene, akt, encoding a serine-threonine kinase containing an SH2-like region. *Science* **254,** 274–277 (1991).

26. Kohn, A. D., Takeuchi, F. & Roth, R. A. Akt, a pleckstrin homology domain containing kinase, is activated primarily by phosphorylation. *J. Biol. Chem.* **271,** 21920–21926 (1996).

27. Garcia-Echeverria, C. & Sellers, W. R. Drug discovery approaches targeting the PI3K/Akt pathway in cancer. *Oncogene* **27,** 5511–5526 (2008).

28. Hennessy, B. T., Smith, D. L., Ram, P. T., Lu, Y. & Mills, G. B. Exploiting the PI3K/AKT pathway for cancer drug discovery. *Nat. Rev. Drug Discov.* **4,** 988–1004 (2005).

29. Ozawa, T., Yoshimura, H. & Kim, S. B. Advances in fluorescence and bioluminescence imaging. *Analytical Chemistry* **85,** 590–609 (2013).

30. Miyawaki, A. Proteins on the move: insights gained from fluorescent protein technologies. *Nature Reviews Molecular Cell Biology* **12,** 656–668 (2011).

31. Frommer, W. B., Davidson, M. W. & Campbell, R. E. Genetically encoded biosensors based on engineered fluorescent proteins. *Chem. Soc. Rev.* **38,** 2833–2841 (2009).

32. Sato, M. & Umezawa, Y. in *Cell Biology, Four-Volume Set* **2,** 325–328 (2006).

33. Morris, M. C. Fluorescent biosensors - Probing protein kinase function in cancer and drug discovery. *Biochimica et Biophysica Acta - Proteins and Proteomics* **1834,** 1387–1395 (2013).

34. Miura, H., Matsuda, M. & Aoki, K. Development of a FRET Biosensor with High Specificity for Akt. *Cell Struct. Funct.* **39,** 9–20 (2014).

35. Sasaki, K., Sato, M. & Umezawa, Y. Fluorescent indicators for Akt/protein kinase B and dynamics of Akt activity visualized in living cells. *J. Biol. Chem.* **278,** 30945–51 (2003).

36. Gao, X. & Zhang, J. Spatiotemporal analysis of differential Akt regulation in plasma membrane microdomains. *Mol. Biol. Cell* **19,** 4366–4373 (2008).

37. Kunkel, M. T., Ni, Q., Tsien, R. Y., Zhang, J. & Newton, A. C. Spatio-temporal dynamics of protein kinase B/Akt signaling revealed by a genetically encoded fluorescent reporter. *J. Biol. Chem.* **280,** 5581–7 (2005).

38. Yoshizaki, H., Mochizuki, N., Gotoh, Y. & Matsuda, M. Akt-PDK1 complex mediates epidermal growth factor-induced membrane protrusion through Ral activation. *Mol. Biol. Cell* **18,** 119–128 (2007).

39. Zhang, L. *et al.* Molecular imaging of Akt kinase activity. *Nat. Med.* **13,** 1114–1119 (2007).

40. Ellis-Davies, G. C. R. Caged compounds: photorelease technology for control of cellular chemistry and physiology. *Nat. Methods* **4,** 619–28 (2007).

41. Kawahama, S. Rapid photolytic release of adenosine 5'-triphosphate from a protected analogue: utilization by the Na:K pump of human red blood cell ghosts. *Tanpakushitsu Kakusan Koso*. **52,** 1772–1773 (2007).

42. Adams, S., Kao, J. P. Y. & Grynkiewicz, G. Biologically useful chelators that release Ca2+ upon illumination. *J. Am. Chem. Soc* **110,** 3212–3220 (1988).

43. Ando, H., Furuta, T., Tsien, R. Y. & Okamoto, H. Photo-mediated gene activation using caged RNA/DNA in zebrafish embryos. *Nat. Genet.* **28,** 317–325 (2001).

44. Leifer, A. M., Fang-Yen, C., Gershow, M., Alkema, M. J. & Samuel, A. D. T. Optogenetic manipulation of neural activity in freely moving Caenorhabditis elegans. *Nat. Methods* **8,** (2011).

45. Deisseroth, K. Optogenetics. *Nat. Methods* **8,** 26–9 (2011).

46. Kennedy, M. J. *et al.* Rapid blue-light-mediated induction of protein interactions in living cells. *Nat. Methods* **7,** 973–5 (2010).

47. Yazawa, M., Sadaghiani, A. M., Hsueh, B. & Dolmetsch, R. E. Induction of protein-protein interactions in live cells using light. *Nat. Biotechnol.* **27,** 941–5 (2009).

48. Bugaj, L. J., Choksi, A. T., Mesuda, C. K., Kane, R. S. & Schaffer, D. V. Optogenetic protein clustering and signaling activation in mammalian cells. *Nat. Methods* **10,** 249–52 (2013).

49. Kim, N. *et al.* Spatiotemporal control of fibroblast growth factor receptor signals by blue light. *Chem. Biol.* **21,** 903–912 (2014).

50. Chang, K.-Y. *et al.* Light-inducible receptor tyrosine kinases that regulate neurotrophin signalling. *Nat. Commun.* **5,** 4057 (2014).

51. Imayoshi, I. *et al.* Oscillatory control of factors determining multipotency and fate in mouse neural progenitors. *Science* **342,** 1203–8 (2013).

52. Wu, Y. I. *et al.* A genetically encoded photoactivatable Rac controls the motility of living cells. *Nature* **461,** 104–8 (2009).

53. Wang, X., He, L., Wu, Y. I., Hahn, K. M. & Montell, D. J. Light-mediated activation reveals a key role for Rac in collective guidance of cell movement in vivo. *Nat. Cell Biol.* **12,** (2010).

54. Nagel, G. *et al.* Channelrhodopsin-2, a directly light-gated cation-selective membrane channel. *Proc. Natl. Acad. Sci. U. S. A.* **100,** 13940–13945 (2003).

55. Boyden, E. S., Zhang, F., Bamberg, E., Nagel, G. & Deisseroth, K. Millisecond-timescale, genetically targeted optical control of neural activity. *Nat. Neurosci.* **8,** 1263–1268 (2005).

56. Ni, M., Tepperman, J. M. & Quail, P. H. Binding of phytochrome B to its nuclear signalling partner PIF3 is reversibly induced by light. *Nature* **400,** 781–784 (1999).

57. Shimizu-Sato, S., Huq, E., Tepperman, J. M. & Quail, P. H. A light-switchable gene promoter system. *Nat. Biotechnol.* **20,** 1041–1044 (2002).

58. Liu, H., Liu, B., Zhao, C., Pepper, M. & Lin, C. The action mechanisms of plant cryptochromes. *Trends Plant Sci.* **16,** 684–91 (2011).

59. Müller, P. & Ahmad, M. Light-activated cryptochrome reacts with molecular oxygen to form a flavin-superoxide radical pair consistent with magnetoreception. *J. Biol. Chem.* **286,** 21033–40 (2011).

60. Idevall-Hagren, O., Dickson, E. J., Hille, B., Toomre, D. K. & De Camilli, P. Optogenetic control of phosphoinositide metabolism. *Proc. Natl. Acad. Sci. USA* **109,** E2316–23 (2012).

61. Kakumoto, T. & Nakata, T. Optogenetic Control of PIP3: PIP3 Is Sufficient to Induce the Actin-Based Active Part of Growth Cones and Is Regulated via Endocytosis. *PLoS One* **8,** (2013).

62. Konermann, S. *et al.* Optical control of mammalian endogenous transcription and epigenetic states. *Nature* **500,** 472–6 (2013).

63. Bergeijk, P. Van, Adrian, M., Hoogenraad, C. C. & Kapitein, L. C. Optogenetic control of organelle transport and positioning. *Nature* **518,** 111–114 (2015).

64. Aoki, K. *et al.* Stochastic ERK activation induced by noise and cell-to-cell propagation regulates cell density-dependent proliferation. *Mol. Cell* **52,** 529–540 (2013).

65. Toettcher, J. E., Gong, D., Lim, W. A. & Weiner, O. D. Light-based feedback for controlling intracellular signaling dynamics. *Nat. Methods* **8,** 837–9 (2011).

66. Milias-Argeitis, A. *et al.* In silico feedback for in vivo regulation of a gene expression circuit. *Nat. Biotechnol.* **29,** 1114–6 (2011).

67. Miyamoto, T. *et al.* Rapid and orthogonal logic gating with a gibberellin-induced dimerization system. *Nat. Chem. Biol.* **8,** 465–70 (2012).

68. Fujita, K. A. *et al.* Decoupling of receptor and downstream signals in the Akt pathway by its low-pass filter characteristics. *Sci. Signal.* **3,** ra56 (2010).

69. Akaike, H. A new look at the statistical model identification. *IEEE Trans. Automat. Contr.* **19,** 716–723 (1974).

70. Zimmermann, S. & Moelling, K. Phosphorylation and regulation of Raf by Akt (protein kinase B). *Science* **286,** 1741–1744 (1999).

71. Burgering, B. M. T. & Medema, R. H. Decisions on life and death: FOXO Forkhead transcription factors are in command when PKB/Akt is off duty. *J. Leukoc. Biol.* **73,** 689–701 (2003).

72. Tran, H., Brunet, A., Griffith, E. C. & Greenberg, M. E. The many forks in FOXO's road. *Sci. STKE* **2003,** RE5 (2003).

73. Nelson, D. E. *et al.* Oscillations in NF-kappaB signaling control the dynamics of gene expression. *Science* **306,** 704–708 (2004).

74. Ashall, L. *et al.* Pulsatile stimulation determines timing and specificity of NF-kappaB-dependent transcription. *Science* **324,** 242–246 (2009).

75. Sandri, M. *et al.* Foxo transcription factors induce the atrophy-related ubiquitin ligase atrogin-1 and cause skeletal muscle atrophy. *Cell* **117,** 399–412 (2004).

76. Stitt, T. N. *et al.* The IGF-1/PI3K/Akt pathway prevents expression of muscle atrophy-induced ubiquitin ligases by inhibiting FOXO transcription factors. *Mol. Cell* **14,** 395–403 (2004).

77. Schiaffino, S., Dyar, K. a, Ciciliot, S., Blaauw, B. & Sandri, M. Mechanisms regulating skeletal muscle growth and atrophy. *FEBS J.* **280,** 4294–314 (2013).

78. Matsuzaki, H. *et al.* Acetylation of Foxo1 alters its DNA-binding ability and sensitivity to phosphorylation. *Proc. Natl. Acad. Sci. USA* **102,** 11278–83 (2005).

79. Higuchi, M., Masuyama, N., Fukui, Y., Suzuki, A. & Gotoh, Y. Akt mediates Rac/Cdc42-regulated cell motility in growth factor-stimulated cells and in invasive PTEN knockout cells. *Curr. Biol.* **11,** 1958–1962 (2001).

80. Kitamura, T. *et al.* Regulation of VEGF-mediated angiogenesis by the Akt/PKB substrate Girdin. *Nat. Cell Biol.* **10,** 329–37 (2008).

81. Enomoto, A. *et al.* Akt/PKB regulates actin organization and cell motility via Girdin/APE. *Dev. Cell* **9,** 389–402 (2005).

82. Chin, Y. R. & Toker, A. The actin-bundling protein palladin is an Akt1-specific substrate that regulates breast cancer cell migration. *Mol. Cell* **38,** 333–44 (2010).

83. Yoshizaki, H., Mochizuki, N., Gotoh, Y. & Matsuda, M. Akt-PDK1 complex mediates epidermal growth factor-induced membrane protrusion through Ral activation. *Molecular biology of the cell* **18,** 119–28 (2007).

84. Miyamoto, Y. *et al.* Akt and PP2A reciprocally regulate the guanine nucleotide exchange factor Dock6 to control axon growth of sensory neurons. *Sci. Signal.* **6,** ra15 (2013).

85. Yoeli-Lerner, M. *et al.* Akt blocks breast cancer cell motility and invasion through the transcription factor NFAT. *Mol. Cell* **20,** 539–50 (2005).

86. Ng, Y., Ramm, G., Lopez, J. a & James, D. E. Rapid activation of Akt2 is sufficient to stimulate GLUT4 translocation in 3T3-L1 adipocytes. *Cell Metab.* **7,** 348–56 (2008).

87. Chung, J., Kuo, C. J., Crabtree, G. R. & Blenis, J. Rapamycin-FKBP specifically blocks growth-dependent activation of and signaling by the 70 kd S6 protein kinases. *Cell* **69,** 1227–1236 (1992).

88. Umeda, N., Ueno, T., Pohlmeyer, C., Nagano, T. & Inoue, T. A photocleavable rapamycin conjugate for spatiotemporal control of small GTPase activity. *J. Am. Chem. Soc.* **133,** 12–14 (2011).

89. Strickland, D. *et al.* TULIPs: tunable, light-controlled interacting protein tags for cell biology. *Nature Methods* **9,** 379–384 (2012).

90. Kawano, F., Aono, Y., Suzuki, H. & Sato, M. Fluorescence imaging-based high-throughput screening of fast- and slow-cycling LOV proteins. *PLoS One* **8,** (2013).

91. Guntas, G. *et al.* Engineering an improved light-induced dimer (iLID) for controlling the localization and activity of signaling proteins. *Proc. Natl. Acad. Sci. U. S. A.* **112,** (2014).

92. Kawano, F., Suzuki, H., Furuya, A. & Sato, M. Engineered pairs of distinct photoswitches for optogenetic control of cellular proteins. *Nat. Commun.* **6,** 6256 (2015).

93. Higuchi, M., Onishi, K., Kikuchi, C. & Gotoh, Y. Scaffolding function of PAK in the PDK1-Akt pathway. *Nat. Cell Biol.* **10,** 1356–1364 (2008).

94. Brandman, O. & Meyer, T. Feedback loops shape cellular signals in space and time. *Science* **322,** 390–5 (2008).

95. Fivaz, M., Bandara, S., Inoue, T. & Meyer, T. Robust neuronal symmetry breaking by Ras-triggered local positive feedback. *Curr. Biol.* **18,** 44–50 (2008).

96. Huang, C. H., Tang, M., Shi, C., Iglesias, P. A. & Devreotes, P. N. An excitable signal integrator couples to an idling cytoskeletal oscillator to drive cell migration. *Nat. Cell Biol.* **15,** 1307–16 (2013).

97. Eyster, C. A., Duggins, Q. S. & Olson, A. L. Expression of constitutively active Akt/protein kinase B signals GLUT4 translocation in the absence of an intact actin cytoskeleton. *J. Biol. Chem.* **280,** 17978–85 (2005).

98. Ali, I. U., Schriml, L. M. & Dean, M. Mutational spectra of PTEN/MMAC1 gene: a tumor suppressor with lipid phosphatase activity. *J. Natl. Cancer Inst.* **91,** 1922–32 (1999).

99. Weiner, O. D. *et al.* A PtdInsP(3)- and Rho GTPase-mediated positive feedback loop regulates neutrophil polarity. *Nat. Cell Biol.* **4,** 509–13 (2002).

100. Wang, F. *et al.* Lipid products of PI(3)Ks maintain persistent cell polarity and directed motility in neutrophils. *Nat. Cell Biol.* **4,** 513–8 (2002).